A MUTATIONAL-FUNCTIONAL ANALYSIS OF THE *ESCHERICHIA COLI* MACRODOMAIN PROTEIN, YMDB

A Thesis Submitted to
The Temple University Graduate Board

In Partial Fulfillment
of the Requirements for the Degree of
MASTERS OF SCIENCE

By
Alexandra Kimberly Smith
December 2018

Examining Committee Members:

Dr. Allen W. Nicholson, Biology and Chemistry (Advisor)

Dr. Richard B. Waring, Biology (Committee Member)

ABSTRACT

A mutational-functional analysis of the *Escherichia coli* macrodomain protein, YmdB

Alexandra Kimberly Smith

Master of Science

Temple University, 2018

Thesis Advisor: Dr. Allen W. Nicholson

Gene expression pathways exhibit many "twists and turns," with theoretically numerous ways in which the pathways can be regulated by both negative and positive feedback mechanisms. A key step in gene expression is RNA maturation (RNA processing), which in the bacterial cell can be accomplished through RNA binding and enzymatic cleavages. The well-characterized bacterial protein Ribonuclease III (RNase III), is a conserved, double-stranded(ds)-specific ribonuclease. In the gram-negative bacterium *Escherichia coli,* RNase III catalytic activity is subject to both positive and negative regulation. A recent study has indicated that an *E. coli* protein, YmdB, may negatively regulate RNase III catalytic activity. It has been proposed that YmdB inhibition of RNase III may be part of an adaptive, post-transcriptional physiological response to cellular stress.

In *E. coli*, the model organism in this study, YmdB protein is encoded by the single *ymdB* gene, and has a predicted molecular mass of ~18.8 kDa. YmdB has been

classified as a macrodomain protein, as it exhibits a characteristic fold that specifically provides an ADP-ribose (ADPR) binding site. While YmdB can bind ADPR with good affinity, there may be additional ligands for the binding site. Thus, YmdB protein may interact with other components in the cell, which in turn could modulate the interaction of YmdB with RNase III.

In previous research conducted within the Nicholson laboratory at Temple University, affinity-purified *Escherchia coli*(*Ec*) YmdB and *Aquifex aeolicus* (*Aa*) YmdB were found to exhibit ribonucleolytic activity. This observation initiated the long-term goal of learning how YmdB regulates RNase III, and how the ribonucleolytic activity of YmdB may be involved in this process. The specific goal of this thesis project was to further characterize the ribonucleolytic activity of *Ec*-YmdB through site-specific mutational analysis. Mutations were introduced into a proposed adenine-binding pocket previously identified by crystallography and by molecular modeling. The adenine-binding pocket is a region within the macrodomain fold where ADP-ribose could bind. The mutations were examined for their effect on *Ec*-YmdB cleavage of a model RNA, R1.1. The results of this study will contribute to the development of a model describing how the ribonucleolytic activity of YmdB is regulated.

ACKNOWLEDGEMENTS

It is with deep gratitude that I would like to thank all those who contributed towards my education in accomplishing the completion of my research. I could not have done this alone without the guidance and encouragement of these my mentors and family. The last two years have given me so many wonderful experiences, new friends here at Temple University and opened up new vistas. A name I will always remember with great regard, is Nicholson.

Dr. Allen Nicholson graciously accepted to be my thesis advisor at a time when I was looking for a laboratory to settle down in and work on a research project. I can never forget the openness with which I was welcomed onto his team. Easily approachable, Dr. Allen Nicholson is the epitome of what one expects as an adviser. His ability to guide the research student, brainstorm as well as explain in depth the problem at hand has been invaluable. I never felt alone during my time working on this research project as he was always available with solutions even when unexpected problems arose. His knowledge of the subject was unmatched as evidenced in discussions after examining new results varying from theoretical expectations. I cannot thank him enough for the care and strong support he gave me as I labored studiously with the goal of learning as much as I could under his tutorship. Dr. Allen Nicholson represents to me everything one expects of a learned professor, and I must express my gratitude in appreciation of success in contributing towards molding and shaping the way I will forever uphold the ethos of

scientific learning and rational thinking. Dr. Allen Nicholson, thank you for all you did for me, in helping me achieve this goal and a step of my life.

I must also say a few words about someone without whom I could not have completed my research work at this time. Dr. Rhonda Nicholson has made immense contributions towards my research, and has taught me the skills I needed to make strides in my work. I learned numerous new laboratory techniques under her gentle and nurturing guidance. Throughout my time in the laboratory, Dr. Rhonda Nicholson was patient and supportive as I learned how to perform new experiments and the tasks leading up to them. Her expertise and patience always gave me a sense of ease and I knew that I would gain new knowledge and go away from the experiment fulfilled. I regard her in high esteem and appreciate her friendship and great advice. She is a wonderful teacher and a wise mentor whom I will greatly miss when I proceed from this great institution in furtherance of my career goals.

Dr. Richard B. Waring, whom I met when I applied for admission into the Master's degree program in the Biology Department here at Temple University. I must have emailed him uncountable times about one thing or the other, and he always responded with an answer. Whatever the problem you threw at him, he always came through with the best solution you could expect. My journey through this program is incomplete without the input I received from Dr. Waring. I always knew whenever I asked him a question or advice that I would receive a direct answer. I thank him very much for all the help he gave me during my work towards completing this program. I cannot thank him fully, I will forever be grateful to him and appreciate his acceptance of my request to serve on my thesis committee.

To Dr. Alex Stopar, I would like to express my deep appreciation to his generosity in assisting me with questions or laboratory techniques. His ready availability to respond to questions or technical issues was invaluable. Having someone readily accessible and willing to answer questions new to me during some of the experiments was a source of support. I always felt comfortable that I could seek help from him. Other professors such as Dr. Joel Sheffield, Dr. Giordano Bellipani and Dr. Rob Kulathinal have contributed in no small measure towards my stay at Temple University.

I cannot complete saying thank you to all those who contributed towards my thesis without mentioning my family. My father Dr. Emmanuel Smith, my mother Kimberly Smith, and my brother Mr. Emmanuel Smith. Without whose continued encouragement, I believe helped me continue to move on. I appreciated that my father understood the intricacies of scientific research and all of the effort that I put into my work, being that he also attended and graduated from this very department under Dr. Frank Chang's direction in 1987. Family can be a source of strength and mine was by supporting me in this endeavor.

Once again, I thank everyone who has contributed towards the pursuit of my educational careers goal.

To my parents, Dr. Emmanuel Smith and Mrs. Kimberly Smith.

TABLE OF CONTENTS

LIST OF FIGURES **Page**

LIST OF TABLE **Page**

CHAPTER 1
INTRODUCTION

1.1 RNA processing, Gene Expression and Genetic Regulation

The central dogma of molecular biology describes the path of gene expression from DNA to RNA transcription and translation into protein. The concept was proposed by Francis Crick in 1970, who asserted that the central dogma refers to deoxyribonucleic acid (DNA) being transcribed into ribonucleic acids (RNA), and where messenger RNAs are then translated into proteins. Therefore, protein is the ultimate product of gene expression. In cooperation with enzymes, DNA copies itself in a process known as genomic replication, allowing transmission of the cells genetic information from generation to generation. Enzymes also are integral to the process by which genetic information stored in the DNA is transcribed into messenger(m) RNA. The mRNA is used as a template for the synthesis of diverse proteins, in a process referred to as translation. Cellular proteins can determine cellular identity and behavior by assisting in the expression of the genetic information, with RNA being an essential intermediary in the process.

DNA in biological systems possesses a double-helical structure, while RNA is commonly single-stranded(ss) (Pray, 2008). The single-stranded nature of RNA allows formation of complex tertiary structures rivaling that of proteins. Often it is complementary base pairing occurring within with same strand of RNA itself that drives the RNA to fold, generating stem-loops and other structures that confer structure and functionality to the RNA, such as enzymatic capabilities (ribozymes), or affinities for certain proteins, metabolites, and other various ligands.

1.1.1 Maturation and Degradation of RNA

There are many modifications that primary RNA transcripts must undergo to become the functional, mature RNA product. In eukaryotic cells, RNA maturation processes include splicing of introns, sequence alterations that can involve deletions, insertions, or even deaminations (editing), as well as "capping" of 5'-ends, polyadenylation of 3'-ends, exonucleolytic cleavage (3'→5' or 5'→3'), endonucleolytic cleavage, and oligouridylation (Alberts 2007, 2002, Lodish 2000). In contrast, modification pathways that contribute to mRNA stability and function have not been identified. Ribonucleases are involved in the exo- and endonucleolytic RNA cleavages in eukaryotic RNA maturation pathways, and they are essential to virtually all RNA degradation pathways in eukaryotes and prokaryotes. RNA concentration levels are regulated in the cell by the rate at which they are transcribed, in association with the rate at which the RNAs are degraded by ribonucleases. Ribonucleases that specifically target the end-most nucleotides at the 3' or 5' terminus are exoribonucleases. Endoribonucleases cleave internal phosphodiester bonds.

1.2 Ribonuclease III

Ribonuclease III (RNase) is an endoribonuclease that preferentially cleaves double-stranded(ds) structures in RNA molecules (Nicholson 2014). The RNase III family includes a functionally and structurally related group of endoribonucleases which have a unique protein fold, referred to as the RNase III (or Nuclease) domain (RIIID or NucD) (Zhang et al. 2004, Kim, Manasherob et al. 2008). This domain is

essential for the RNase III family's cleavage activity as it contains the highly conserved amino acids that play essential roles in the enzyme's catalytic action towards dsRNA. The domain consists of ~150 amino acids that is primarily α-helical (Nicholson 2014). RNase III requires a divalent metal ion such as Mg^{2+} to hydrolyze phosphodiester linkages within dsRNA (Nicholson 2014). This study used recombinant E. coli RNase III. E. coli RNase III is involved in RNA maturation and degradation pathways, host defense against viral infection, and gene regulation (Nicholson 2003).

1.3 The Macrodomain protein, YmdB

1.3.1 The Macrodomain

The macrodomain is a name given to a highly conserved protein fold that is seen in proteins in Bacteria, Eukarya, Archaea, and viruses (Chen, Vollmar et al. 2011). Macrodomains are known for their structural and mechanical stability (Guzman, et al. 2010), and have exhibited a slow rate of evolution (Li, Wu et al. 2013). Macrodomain proteins are involved in a range of biological functions including regulation of the cellular response to DNA damage, transcription, chromatin remodeling, and tumorigenesis, (Han, Li et al. 2011, Li, Wu et al. 2013). Though macrodomains are highly conserved, the slight variations identified within their sequences play key roles in establishing protein function (Han, Li et al. 2011). Macrodomain-containing enzymes catalyze the post-translational modification termed ADP-ribosylation. NAD^+ is used as a cosubstrate to transfer multiple or single ADP-ribose (ADPR) moieties onto the target proteins. A cell under stress,

with, for example, DNA damage, can carry out this reaction as part of the DNA repair pathway (Jankevicius, Hassler et al. 2013).

An important protein modification is the acetylation of lysine. Indeed, the activities of specific lysine-acetylated proteins can be regulated *via* deacetylation. This reaction is performed by sirtuins, with catalysis achieved in an NAD^+-dependent manner (Tong and Denu 2010). The NAD^+-dependent deacetylation reaction performed by sirtuins produces O-acetyl-ADP-ribose (OAADPR) as a product, along with the deacetylated protein (Tong and Denu 2010). In this reaction the glycosidic bond within the nicotinamide ribose moiety is cleaved, producing nicotinamide and OAADPR (where the ribose 2'-OH or 3'-OH group accepts the acetyl group from the protein substrate) (Tong and Denu 2010). The intracellular levels of ADPR and OAADPR have been associated with metabolic shifts that decrease the production of endogenous reactive oxygen species, in addition to diverting glucose and preventing oxidative damage (Tong and Denu 2010). It has been proposed that OAADPR could potentially hold an important function as a signaling molecule as well as functional substrate for enzymatic processes downstream from sirtuin reactions (Tong and Denu 2010).

In humans, there are at least eleven different macrodomain proteins that are encoded by ten genes (Peterson et al. 2011, Han, Li et al. 2011, Kraus 2009, Neuvonen and Ahola 2009). Several of the macrodomain proteins function as OAADPR deacetylases, and are termed MacroD-like proteins. These include the human MacroD1 and MacroD2 proteins, the sirtuin-linked SAV0325 protein of *Staphylococcus aureus*, and *E. coli* YmdB (Peterson et al. 2011, Chen, Vollmar et al. 2011). MacroD1,

MacroD2 and C6orf130 proteins bind ADPR (Fig. 1) The macrodomain exhibits a characteristic groove that binds ADPR as well as related metabolites such as OAADPR, and consists of ~130-190 amino acids (Chen, Vollmar et al. 2011, Han, Li et al. 2011) (Fig. 1). The two human macrodomain proteins MacroD1 and MacroD2 are homologous to each other in both structure and function, and are highly similar to bacterial YmdB proteins (Peterson et al. 2011).

OAADPR can bind to the macrodomain of splice variants of MacroH2A, a histone protein that is enriched within regions of heterochromatin (Tong and Denu 2010). This suggests a direct involvement of OAADPR on gene expression, chromatin remodeling, or DNA repair (Tong and Denu 2010). ADPR is involved with the stress response, gated ion channel function, cellular longevity, and regulation of transcription as a signaling molecule (Huang, De Ingeniis et al. 2009). These metabolites and conceivably others related to them, play essential roles in cellular function. Finally, elevated cellular concentrations of ADPR provides an indicator of NAD^+ subjected to active turnover (Huang, De Ingeniis et al. 2009).

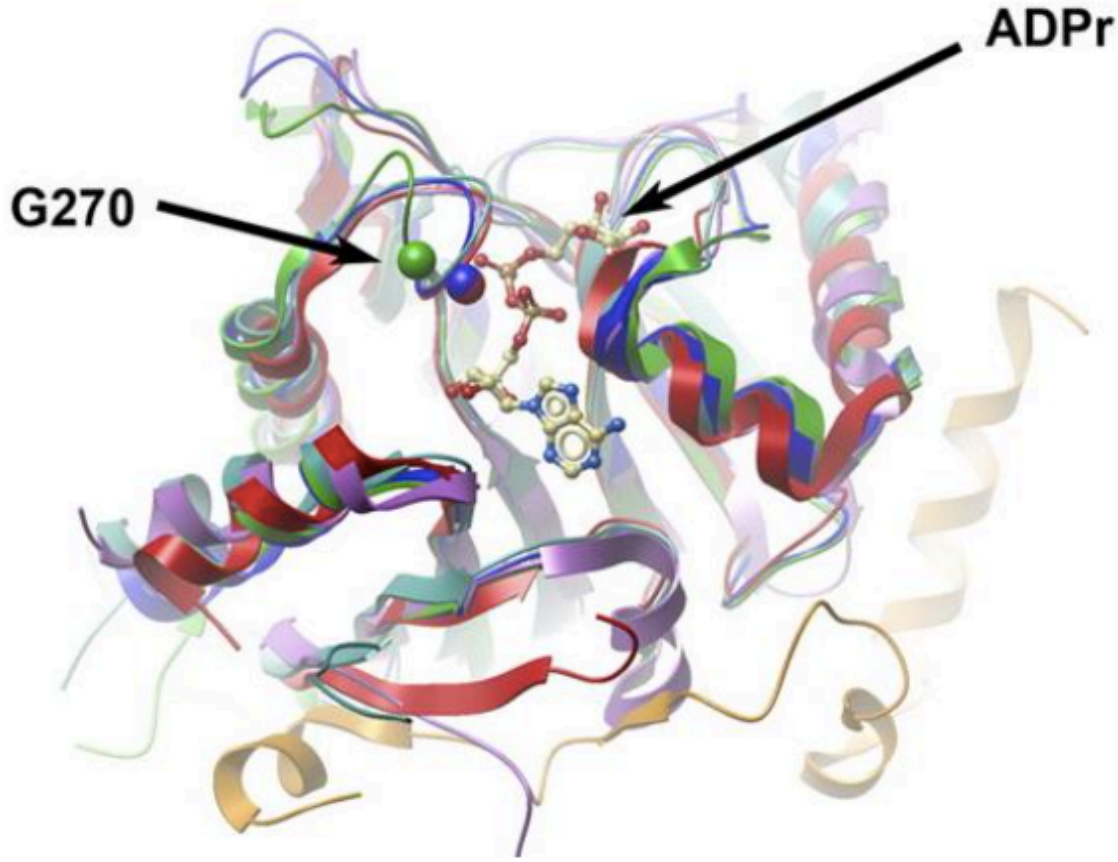

Figure 1. Crystallographic structure overlay of specific macrodomain proteins (Chen, Vollmar et al. 2011)

A ribbon structure for MacroD1 (orange and green) is superimposed on the macrodomains of *E. coli* YmdB (blue) (PDB ID: 1SPV), Feline sarcoma virus (purple) (PDB ID: 3KH6), and histone macroH21.1 (red) (PDB ID: 3IID). Centrally located within the structure of the diagram is an ADP-ribose (ADPR) atomic model that is associated with the Feline sarcoma virus. The G270 residue in MacroD1 (blue and green spheres) is involved in ADPR binding, with G124 being the equivalent residue in *E. coli* YmdB . The phosphate(P)-binding loop (P-loop) includes the G270 residue, giving access to interact with the pyrophosphate moiety of ADPR. The G124E mutation Ec-YmdB inhibits OAADPR hydrolysis and blocks ADPR binding (Chen, Vollmar et al. 2011, Kustatscher, Hothorn et al. 2005).

1.3.2 YmdB structure and function

E. coli(*Ec*) YmdB acts as an OAADPr deactylase; the protein catalyzes the deacetylation of OAADPr yielding acetate and ADP-ribose (Peterson et al. 2011, Chen, Vollmar et al. 2011). In response to specific cellular stress such as cold shock, YmdB levels increase (Kim, Manasherob et al. 2008). As the YmdB concentration rises there is a decrease in RNase III catalytic activity (Kim, Manasherob et al. 2008). Prior to this observation, an *E. coli* protein was identified with a molecular mass ~17kDa that was able to inhibit *Ec*-RNase III cleavage of dsRNA *in vitro* (Makarov and Apirion 1992). Subsequently, Stanley Cohen and colleagues identified a protein of similar molecular mass, ~18.8 kDa (Kim, Manasherob et al. 2008). Identified as a macrodomain protein, YmdB was capable of only weak inhibition of RNase III *in vitro* (Kim, Manasherob et al. 2008). *In vivo*, YmdB has been found to down-regulate RNase III in a dose-dependent manner (Kim, Manasherob et al. 2008). Upon cell entry into stationary phase, or during cold-shock, the *ymdB* gene experiences transcriptional enhancement (Kim, Manasherob et al. 2008). Overexpression of YmdB inhibits E. coli biofilm formation and has an effect on the expression of over 2,000 genes (Kim, Lee et al. 2013). Of these 2000 genes, 129 are strongly regulated by YmdB. Of these 129 genes, 80 are not RNase III targets (Kim, Lee et al. 2013). Additionally, 10 genes strongly influenced by YmdB, play a role in biofilm formation (Kim, Lee et al. 2013). Biofilm formation is, therefore, regulated interdependently by both YmdB and the known stress response regulator, RpoS (Kim, Lee et al. 2013).

As mentioned above, the macrodomain protein YmdB has an ADPR binding site that is highly conserved. The structure of this macrodomain region within

Ec-YmdB shares a strong resemblance with that of the Chikungunya virus (CHIKV) macrodomain protein, nsP3 (Fig. 2). The CHIKV nsP3 protein is part of a viral replication complex, and is highly phosphorylated (Fros et al. 2012). The nsP3 protein, similar to YmdB, has a conserved adenine-binding pocket (Malet et al. 2009). Previous computational and modeling studies from the Nicholson laboratory at Temple University identified residue D160 of *Ec*-YmdB to potentially have an involvement with *Ec*-YmdB ribonucleolytic activity. Residue D160 is near the adenine-binding pocket. It was shown that the D160A mutation supports *Ec*-YmdB ribonucleolytic activity at elevated salt concentrations that would otherwise inhibit activity in the wild-type *Ec*-YmdB.

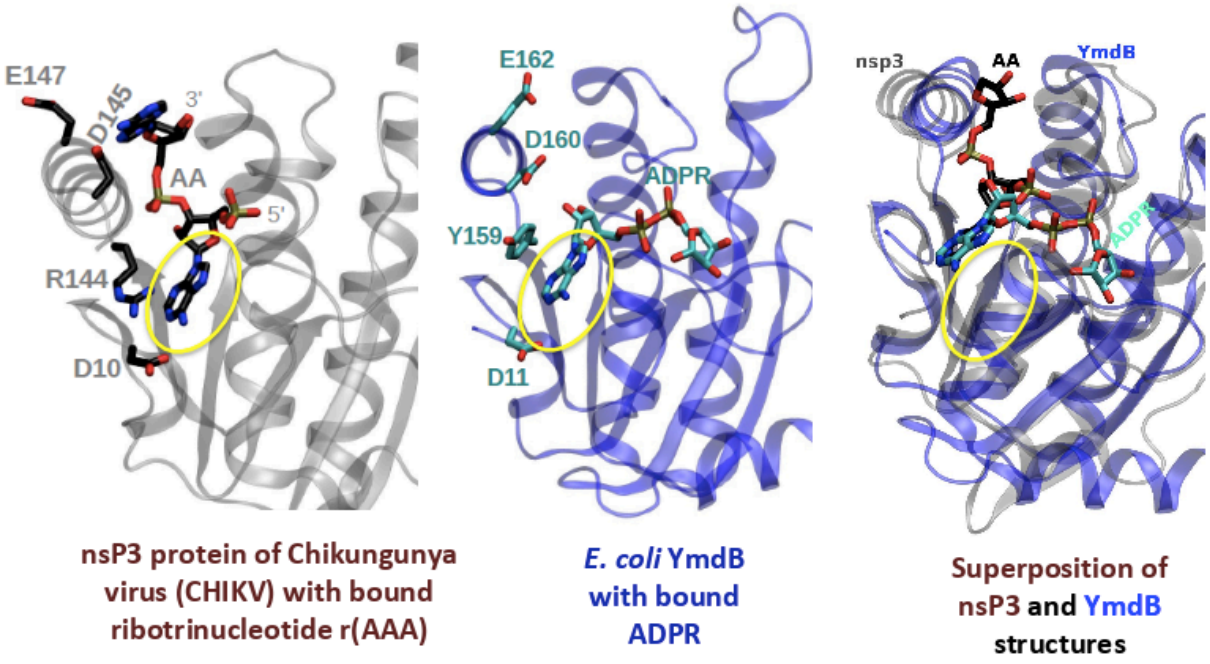

Figure 2. ADPR and RNA recognition involves the macrodomain adenine-binding pocket. (Source: Dr. M. Alfonso-Prieto, ICMS, Temple University) (*Left panel*) Ribbon structure (grey) of nsP3 protein from Chikungunya virus (CHIKV) bound to the ribotrinucleotide, r(AAA). Only "AA" is indicated, in reference to the 3' nt and the middle nt, as the third 5'-end A residue cannot be observed. The R144 and D10 residues play important roles in adenine specificity and binding affinity. (*Center panel*) Ribbon structure (purple) of *E. coli* YmdB bound to ADPR. Residues Y159 and D11 are equivalent to residues R144 and D10 of nsP3. Residues E162 and D160 in *Ec*-YmdB are equivalent to nsp3 residues E147 and D145, respectively. E162 and D160 are locted in the C-terminal helix, in close proximity to the ADPR binding site in *Ec*-YmdB. (*Right panel*) Superimposed crystallographic structures of Ec-YmdB and CHIKV nsP3 protein. The central adenine of the rAAA, and the adenine of ADPR bind to the adenine-binding pocket.

1.3.3 YmdB regulation of RNase III

YmdB and RNase III interact *in vivo*, based upon a mass spectrometry analysis of the *E. coli* protein interactome. YmdB also interacts with D-allose kinase (DAK) (Butland, Peregrin-Alvarez et al. 2005; Hu, Janga et al. 2009). Ec-YmdB is a stress-responsive regulator of RNase III ribonucleolytic activity (Kim, Manasherob et al. 2008, Kim, Lee et al. 2013). When YmdB levels increase in response to stress inputs, RNase III catalytic activity decreases. The inhibitory mechanism has not been determined. RNase III activity is down-regulated during cold-shock and cell entry into stationary phase (nutrient deprivation). RNase III downregulation is correlated with YmdB production during cold-shock, although downregulation still occurs in *ymdB*-null mutant bacteria (Kim, Manasherob et al. 2008, Kim, Lee et al. 2013). Previous experiments from the Nicholson laboratory at Temple University found that both *E. coli* and *A. aeolicus* YmdB exhibit ribonucleolytic activity, independent of RNase III (Paudyal, 2014). The ribonucleolytic mechanism and the residues important for RNA cleavage have not been elucidated.

1.4 Research objectives

The long-term goals are to determine the mechanism of YmdB regulation of RNase III, and define the involvement of YmdB ribonucleolytic activity in bacterial cell RNA metabolism. The objective of this project has been to focus on the involvement of the adenine binding pocket on the ribonucleolytic activity of *Ec*-YmdB. The experimental approach was to create Ec-YmdB mutants with altered adenine-binding pockets, and assess ribonucleolytic activity in vitro. A testable hypothesis is that the adenine-binding pocket binds adenine residues in RNA

substrates, which then allows cleavage of an adjacent phosphodiester. As shown below, the experimental results do not support this model, but instead suggest an alternative function for the adenine-binding pocket.

CHAPTER 2
MATERIALS AND METHODS

2.1 Materials and Reagents

2.1.1 Materials

Double-distilled, deionized water was used for all buffers and solutions. Microcentrifuge tubes and pipette tips were obtained from BioExpress (Kaysville, UT). Molecular biology grade reagents and chemicals were acquired from Millipore-Sigma (Saint Louis, MO) or ThermoFisher (Chicago, IL). Whatman 3M filter paper, Fuji Super RX film, and Spectra-por dialysis membranes with 10 kDa molecular weight cut-off were obtained from ThermoFisher. Ni^{2+}-NTA chromatography (HisBind) resin was purchased from Novagen, and Amicon spin concentrators for protein concentration were purchased from EMD Millipore (Billerica, MA). The standardized 1M $MgCl_2$ solution was obtained from Millipore-Sigma. Combs, spacers, and glass plates used to make the polyacrylamide gels for electrophoresis were purchased from LabRepCo (Horsham, PA). The 1 ml His Trap™ FF crude column and 5 ml HiTrap™ Desalting column were purchased from GE Healthcare Life Sciences (Piscataway, NJ). Ribonucleoside 5'-triphosphates (rNTPs) for the transcription reactions were obtained from SigmaAldrich. Plasmid purification kits were purchased from Qiagen (Valencia, CA). Perkin-Elmer (Boston, MA) supplied the RNA radiolabeling reagent [α-^{32}P]UTP (3000 Ci/mmol). T7 RNA polymerase was purified in the Nicholson laboratory as described (He et al. 1997). Molecular biology grade glycerol for cell storage and enzymatic assays was purchased from Sigma. ThermoFisher supplied the sterile petri dishes, loops, spreaders, as well as polypropylene and polystyrene tubes for cell cultures. NuPAGE 12% Bis-Tris Gel (1.0mm x 10 well) was purchased from Novex/Invitrogen. Protein molecular weight markers were purchased from Bio-Rad Laboratories (Hercules, CA). Integrated DNA Technologies synthesized

oligodeoxynucleotide transcription templates and mutagenic oligodeoxynucelotides. Purified DNA was always stored at -20°C in TE buffer (pH 8.0).

2.1.2 Buffers and Reagents

The pH of all buffers was adjusted when a specific value was required. Specifically, the Tris buffers were adjusted by addition of 12N HCl. In contrast, the pH for stock solutions of EDTA were adjusted by adding NaOH pellets, or aliquots of a 1M NaOH solution. All inorganic salt solutions and Tris buffers were autoclaved.

TE Buffer (1X)

10 mM Tris-HCl (pH 8.0)

1 mM EDTA (disodium salt)

TBE Buffer (10X) (no pH adjustment is required; pH 8.0-8.2)

890 mM Tris base

890 mM Boric acid

20 mM EDTA (disodium salt)

TAE Buffer (10X) (no pH adjustment is required; pH 8.0-8.2)

400 mM Tris base

200 mM Glacial acetic acid

10 mM EDTA disodium salt (added from a 0.5 M, pH 8.0 stock solution)

DNA/RNA Extraction Buffer (pH 8.0; adjusted with use of NH_4OH)

500 mM Ammonium acetate

10 mM EDTA disodium salt (from a 0.5 M stock solution, at pH 8.0)

LB Agar plates with Ampicillin (recipe for 500 ml)

17.5g LB Agar

500 ml ddH_20

100 μg/ml Ampicillin

*The ampicillin solution is only added after the autoclaved LB agar solution is cooled to ~37 °C on the lab benchtop, the solution is then poured into the plates.

LB broth (500ml)

12.5g LB broth

500 ml ddH_20

*Follow by autoclaving for ~25 minutes

Protein Dilution Buffer 1A (1X)

30 mM Tris-HCl (pH 8.0)

0.1 mM DTT

0.1 mM EDTA disodium salt (from a 0.5 M stock solution, at pH 8.0)

Protein Dilution Buffer 1B (1X) [used for protein suspended in 150mM NaCl storage buffer)

30 mM Tris-HCl (pH 8.0)

75 mM NaCl

0.1 mM DTT

0.1 mM EDTA disodium salt (from a 0.5 M stock solution, at pH 8.0)

Reaction Stop Solution / Denaturing Gel Loading Solution (2X)

89 mM Tris base

89 mM Boric acid

40 mM EDTA (disodium salt) (from a 0.5 M stock solution, at pH 8.0)

10% (v/v) Glycerol (Molecular Biology Grade)

7M Urea

20% (w/v) Sucrose (optional)

0.04% (w/v) Xylene cyanol

0.04% (w/v) Bromophenol blue

Bacterial Cell Cracking Buffer (1X) for SDS-PAGE

50 mM Tris HCl (pH 6.8)

20 mM EDTA (disodium salt)

10% (v/v) Glycerol

1% (v/v) 2-mercaptoethanol

1% (w/v) SDS

SDS Gel MES-Running Buffer (1X) pH 7.5

50 mM MES (sodium salt)

50 mM Tris base

0.1% (w/v) SDS

1 mM EDTA disodium salt

Gel Staining Buffer

45% (v/v) Methanol

10% (v/v) Glacial Acetic Acid

0.1% (w/v) Coomassie Brilliant Blue R-250

Gel Destaining Buffer

45% (v/v) Methanol

10% (v/v) Glacial Acetic Acid

(2x) Denaturing Gel Loading Buffer

100 mM Tris-HCl (pH 6.8)

4% (w/v) SDS

0.2% Bromophenol Blue

20% glycerol

200mM DTT (added fresh each time before use)

Ni^{2+} - NTA column Binding Buffer

20 mM Tris-HCl (pH 8.0)

500 mM NaCl

5 mM Imidazole

1 mM Tris(2-carboxyethyl)phosphine (TCEP) [Reducing agent added upon usage]

Bio-Rad Colorimetric Protein Assay Solution

1 ml concentrated Bio-Rad Protein Assay Solution

4 ml distilled, deionized H_2O

Precisions Plus Protein™ Dual Xtra Standard cat. No. 1610377

Ni^{2+} - NTA (HisBind) column Elution Buffer

20 mM Tris-HCl (pH 8.0)

500 mM NaCl

400 mM Imidazole

1 mM TCEP [Reducing Agent added upon usage]

Ni^{2+} - NTA column Wash Buffer

20 mM Tris-HCl (pH 8.0)

500 mM NaCl

60 mM Imidazole

Ni^{2+} - NTA column Dialysis Buffer (Buffer A)

60 mM Tris-HCl (pH 8.0)

500 mM NaCl

200 mM Imidazole

Ni^{2+} - NTA column Dialysis Buffer (Buffer B)

60 mM Tris-HCl (pH 8.0)

500 mM NaCl

1 mM EDTA (disodium salt) (from a 0.5 M stock solution, at pH 8.0)

1 mM DTT

Protein Storage Buffer

[following desalting]

20 mM Tris-HCl (pH 8.0)

150 mM NaCl

1 mM TCEP [Reducing Agent added upon usage]

Ni^{2+} - NTA column Stripping Buffer

20 mM Sodium phosphate

500 mM NaCl

50 mM EDTA (disodium salt; pH 7.4)

Ni^{2+} - NTA column Recharge Solution

100 mM $NiSO_4$

T7 RNA Polymerase Transcription Buffer (1X)

40 mM Tris-HCl (pH 8.0)

20 mM $MgCl_2$

10 mM spermidine

5 mM DTT

0.01% Triton X-100

Stop Mix for YmdB Cleavage Reactions / SDS PAGE Sample Buffer (4X)

40% Glycerol

4% SDS (a decrease to 1% improves RNA electrophoresis)

100 mM Tris-HCl (pH 7.5)

2 mM EDTA (disodium salt) (from a 0.5 M stock solution, at pH 8.0)

0.050% Bromophenol Blue

***E. coli* RNase III Substrate Cleavage Assay Buffer (1X)**

30 mM Tris-HCl (pH 8.0)

160 mM NaCl

10 mM $MgCl_2$ (added to initiate RNA cleavage reactions)

30% Acrylamide Stock Solution (36.5:1; acrylamide: bisacrylamide)

(used for preparing denaturing polyacrylamide gels for RNA electrophoresis)

29% (w/v) Acrylamide

1% (w/v) N, N'-methylene-bisacrylamide

15% Polyacrylamide Gel / 7M Urea (for the substrate cleavage assays) ~35ml

21 g Urea

5 ml (10X) TBE

15 ml 30% Acrylamide Stock solution (36.5:1) (see above)

0.5 ml 10% (w/v) Ammonium persulfate

0.05 ml TEMED (added last, just before pouring into frame)

2.1.3 Bacterial Strains

The *E. coli* strains utilized for this project were XL-10 Gold Ultracompetent cells; NEB 10-beta (a DH10B derivative); and BL21(DE3). Cell stocks were stored at –80°C.

XL-10 Gold Ultracompetent cells (Agilent Technologies) were used for site-specific mutatgenesis and have high transformation efficiencies. High-quality plasmid DNA for sequencing can be isolated from this strain since it contains the *endA1* allele that suppresses DNA endonuclease activity. These cells also are capable of suppressing plasmid recombination, as they carry the *recA* allele. The XL-10 Gold Ultracompetent cells have resistance against tetracycline and chloramphenicol, due to the two genes, Tet^R and Cam^R, respectively.

NEB 10-beta cells, a derivative strain of DH10B, are resistant to phage T1infection due to the *fhuA2* allele. These cells were used for plasmid cloning. A wide variety of antibiotics can be used for plasmid selection, including ampicillin, carbenicillin, chloramphenicol, kanamycin, and tetracycline. Ampicillin was used throughout the experiments performed for this project. These cells also carry the *recA*1 allele, reducing the recombination of cloned DNA. The NEB 10-beta cells have eliminated the activity of nonspecific endonuclease I, yielding the highest quality plasmid preparations.

BL21(DE3) cells were used for overexpression of recombinant wild-type and mutant proteins. They have the genetic element DE3, which contains the T7 RNA polymerase gene under control of the IPTG-inducible *lacUV5* promoter. These cells are deficient in proteases OmpT and Lon, which improves the quality of purified proteins. Additionally, these cells are phage T1 (*fhuA2*) resistant, and a broad assortment of

antibiotics can be used for plasmid selection, including ampicillin, carbenicillin, chloramphenicol, kanamycin, streptomycin and tetracycline. Ampicillin was used throughout the experiments performed in this project.

A

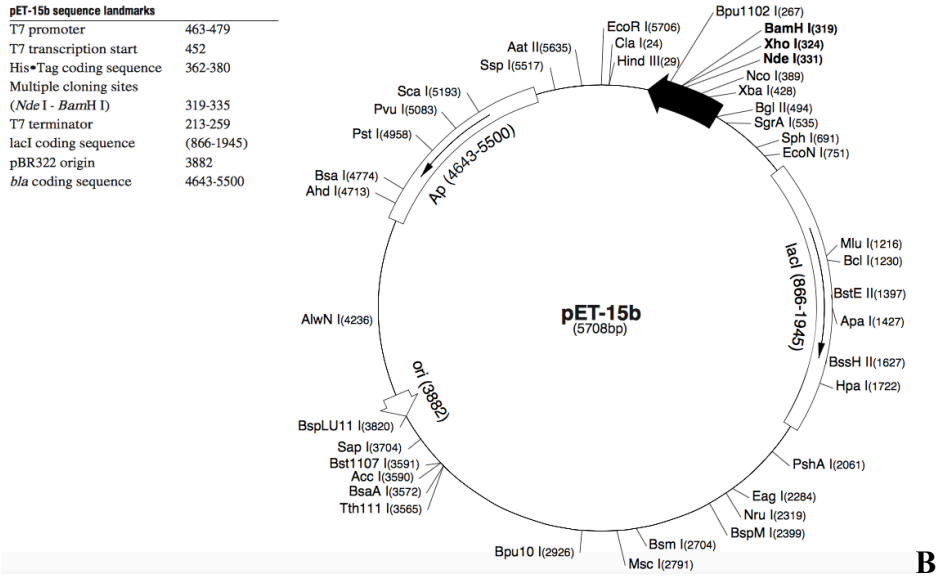

B

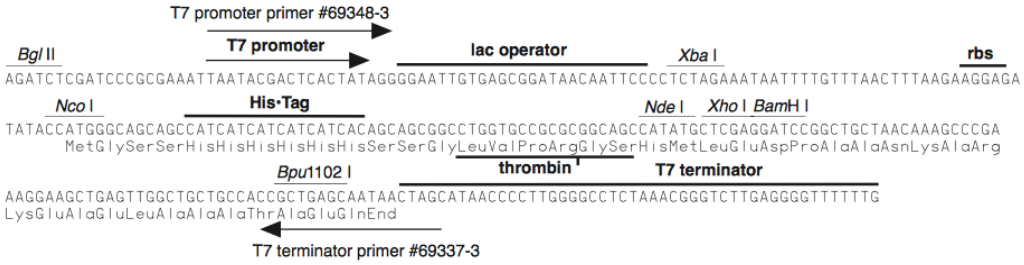

pET-15b cloning/expression region

Figure 3. Important genetic elements and the cloning/expression region shown on the physical and genetic map of plasmid pET-15b.

A. Plasmid pET-15b encodes an N-terminal hexahistidine-tag sequence, followed by a thrombin cleavage site and multiple cloning site (Novagen). The locations of the origin of replication (ori), lactose repressor gene (lacI), and Ampicillin-resistance gene (Ap) are indicated by arrows. The legend on the left highlights additional pET15-b genetic elements. B. This figure accentuates the T7 promoter, hexahistidine tag, lac operator, thrombin cleavage site, multiple cloning site, and T7 transcription termination sequences within a specific region of the pET-15b plasmid.

The *ymdB* gene was cloned into the pET-15b plasmid. *E. coli* XL-10 Gold Ultracompetent cells were used for creating mutations in the cloned sequence. Growth and purification of the pET-15b(*ymdB*) plasmid was achieved using the *E. coli* NEB 10-beta cells. Overexpression and purification of wild-type and mutant *Ec*-YmdB was accomplished by the *E. coli* BL21 (DE3) cells.

2.2 Methods utilized for biochemical experiments and analysis.

2.2.1 Preparation of recombinant plasmids for protein overexpression

The controlled overexpression of recombinant protein in high yield is made possible with the pET plasmid collection (Novagen) (Fig. 3). In this project, a sample of genomic DNA was used to amplify the wild-type Ec-ymdB gene by the polymerase chain reaction. The Ec-ymdB gene was cloned into the Nde1 and BamHI sites in the multiple cloning region of plasmid pET-15b, downstream of the T7 promoter region.

The *lac*O (lac operator)-*LacI* (lac repressor) system control the T7 promoter in pET15b. An N-terminal $(His)_6$-tag sequence (~2 kDa) is encoded by the pET-15b plasmid, followed by a thrombin cleavage site. The Nde1 and BamHI cloning sites are downstream and in frame with the $(His)_6$-tag sequence and the thrombin cleavage site. An ampicillin resistance gene and T7 transcription terminator sequence are also genetic components of pET-15b.

2.2.1.1 Transformation of Plasmids and Purification

For transformation of *E. coli* NEB 10-beta cells, electrocompetent cells stored at minus 80°C were allowed to thaw on ice for ~10 min. The specific purified plasmid of interest (~100ng in 1 µl) was then gently mixed with 20 µl of the thawed cells, and incubated for 30 min on ice. The solution was then heat shocked for exactly 30 seconds at

precisely 42°C, while also making sure to not disturb the cells. The cells were then placed on ice for 5 minutes without mixing. 950 µl of room-temperature NEB 10-beta/Stable Outgrowth Medium (no antibiotic) was then added to the mixture. The cell culture was then placed at 37°C and allowed to vigorously shake for 1 hour at ~250 rpm. 100-250 µl of the culture was spread on a pre-warmed (37°C) LB agar selection plates with ampicillin (100 µg/ml). The plates were then incubated overnight at 37°C.

An individual colony was chosen from the selection plate, inoculated into a 10 ml culture in LB medium with ampicillin (100 µg/ml), and allowed to shake vigorously overnight at 37°C. The 10 ml culture was then centrifuged at 6000 x *g* for 15 minutes. The plasmid was purified using the Qiagen Plasmid Mini Kit (cat. No. 12123 and 12125) following the supplier's protocol. Gene Wiz sequenced the plasmid inserts according to their instructions, and using a T7 promoter oligonucleotide as sequencing primer.

2.2.1.2 Site-directed Mutagenesis

The Quick-Change Lightning Site-directed Mutagenesis kit (Agilent Technologies) was used for site-directed mutagenesis. The DNA template was the sequence-confirmed Ec-ymdB gene cloned in pET-15b. The mutagenic oligodeoxynucleotides incorporated a design that provided a Tm (melting temperature) for the duplex at ~80°C, with the GC (Guanine and Cytosine) and AT (Adenine and Thymine) content each at ~50%. (Table I) .

2.2.2 Protein overexpression and purification

E. *coli* BL21(DE3) cells were used to overexpress the *Ec*-YmdB polypeptides for this project.

2.2.2.1 Protein overexpression

To achieve *Ec*-YmdB protein production, the pET-15b recombinant plasmid was transformed into BL21(DE3) cells through heat shock at 42°C. The high efficiency transformation protocol detailed by New England BioLabs, the provider of the BL21(DE3) cells, was followed to produce a strong transformation. Chemically competent BL21(DE3) cells are stored at -80°C, and are thawed just before use on ice for 10 min. From the vials containing 50 µl of BL21(DE3) cells, a 20 µl aliquot is removed and pipetted into a separate sterile tube. 1 µl of plasmid DNA(~100ng) is then added to the mixture of cells set aside on ice; the tube containing the cell and DNA mix are gently flicked 4-5 times to ensure that the DNA is evenly spread across the cells. The mixture is then placed on ice for 30 min without further mixing. The cell mixture was then heat shocked precisely at 42°C for 10 seconds, making sure to not disturb the cells. Next the solution was kept on ice for 5 min. 950 µl of room temperature SOC medium was pipetted into the cells, and the culture was incubated with vigorous shaking for 1 hour at 37°C. Afterwards the cell mixes were flicked and inverted, spreading ~150-250 µl of the mix onto pre-warmed (~37°C) LB agar selection plates, which contained ampicillin (100 µg/ml). The selection plates were incubated overnight at 37°C, or to the point that the colonies had grown to a suitable size. An individual well-defined colony was picked and inoculated into 10 ml of LB broth medium with ampicillin (100 µg/ml), and incubated at 37°C overnight. A 2.8 L Erlenmeyer flask containing 500 ml of LB-broth with ampicillin (100 µg/ml) was then inoculated with the overnight culture, followed by incubation with shaking (~225-250 rpm) at 37°C for several hours until the cells grew to the point at which the optical density reached ~0.4, at a wavelength of 595 nm). Isopropyl β-D-1-

thiogalactopyranoside (IPTG) then was added to a final concentration of 1 mM, inducing expression of the T7 polymerase. The T7 polymerase then transcribed the recombinant ymdB gene. (Constant transcription of the ymdB gene by T7 polymerase leads to protein overexpression in the BL21(DE3) cells.) Cell cultures were then allowed to continue incubation for ~4-6 hours. In order to verify overexpression of the ymdB gene, a 1 ml aliquot was taken just prior to IPTG addition and also ~4 hours after IPTG addition. These samples were saved for analysis on a denaturing polyacrylamide gel. The 500 ml culture was split into two collection bottles, each containing 250 ml of the cell culture. The cells were pelleted by centrifugation at 6000 rpm and 4°C in a Sorvall RC6+ for 20 minutes. The supernatant was decanted from all of the bottles. One bottle with a cell pellet was stored at -20°C for immediate use, while the other was placed at -80°C for long-term storage and future analyses.

The 1 ml aliquots of cells taken just prior to, and ~4 hours following IPTG addition were analyzed for YmdB protein overexpression. The 1 ml aliquots were centrifuged for 10 min at 5000 rpm, then heated for ~10 min in SDS cracking buffer at ~90°C. At this point the culture was mixed well with a pipette, then kept at -20°C overnight if necessary. Aliquots were thawed on ice and ~5-10 µl of the sample was mixed with an equal volume of Reaction Stop Mix / 2X Denaturing Gel Loading Buffer (containing bromophenol blue). Samples were heated using an Applied Biosystems Thermal Cycler for 20 min (70°C for 10 min, followed immediately by 25°C for 10 min). The ~10-20 µl sample was then analyzed by electrophoresis in a 12% Bis-Tris NuPAGE minigel (Life Technologies) at a constant voltage of ~120V. The gel was placed in staining buffer and subjected to gentle rocking on an Orbitron rotator II (Model 260250,

Boekel Scientific) for ~1 hour. The staining buffer was decanted, replaced with destaining buffer, and rotation continued for 1 hour. The spent destaining buffer was decanted and replaced with fresh destaining buffer. Destaining continued on the rotator overnight.

2.2.2.2 Protein Purification

The recombinant proteins analyzed in this study contained an N-terminal $(His)_6$ affinity tag, which was encoded by the pET-15b expression plasmid. This tag allowed the protein to be purified by affinity chromatography using a Ni^{2+}-NTA column. Proteins were purified by three different methods, providing varying degrees of purity.

2.2.2.2.1 Ni^{2+}-NTA affinity purification of protein

IPTG-treated *E. coli* BL21(DE3) cells carrying recombinant pET-15b plasmids were harvested from ~250 ml of culture and resuspended in ~20 ml of Ni^{2+}- column binding buffer. The solution was thoroughly swirled to ensure complete solution of the pellet, and then was poured into a 100 ml beaker on ice. The mixture was subjected to repetitive ultrasonic pulses (1 min, 5-6 watts; Misonix Inc), with cooling periods of 1 min in between, keeping the beaker in ice. This was continued until the solution became homogenous (~20-35 min). Low speed centrifugation (20-30 min at 6000 rpm, 4°C) was then used to clarify the sonicated solution. The supernatant was then carefully collected slowly with a pipette, making sure to leave a little bit of liquid over the pellet, so as not take up any of the solid material at the bottom of the tube. The supernatant was then applied to an affinity purification column. To prepare the Ni^{2+}-NTA column, a 25 ml disposable plastic pipette was shortened, and a small, wadded ball of sterilized glass wool was gently pushed down to the tip of the pipette to act as

a support for the resin. The column is clamped vertically onto a sturdy metal stand inside of a refrigerated dairy case at a 4°C. This set-up allows buffers to flow through the column by gravity. HisBind resin (~1.5 ml) (Novagen) was added to the shortened pipette; it then settles atop the glass wool plug. A short (~3") section of Tygon tubing is attached to the end of the pipette tip, and is used to direct the flow of the eluent and ensure it goes into the proper collection tubes. To control and maintain column flow rate of ~1ml/min, a small screw-clamp can be fastened onto the tygon tubing. Prior to loading the sample, the column is washed with ~10 ml of Ni^{2+}- NTA column binding buffer, then charged with ~10 ml $NiSO_4$ [50 mM]. The clarified supernatant is then loaded on to the column. (Note: Buffer added to the column should be allowed to flow through until ~0.5 ml remains. At this point, the subsequent buffer can be poured onto the column. The HisBind resin must not dry out). Once the sample has run through the resin, the column is washed with Ni^{2+}-NTA binding buffer (30 ml), followed by Ni^{2+}-NTA column washing buffer (40 ml) in order to remove additional impurities or proteins that are still on the resin. 10 ml of Ni^{2+}-NTA elution buffer was added to the column and 1 ml fractions of eluent were collected in 1.7 ml polypropylene microcentrifuge tubes. To check which fraction contained eluted protein, a 20 µl aliquot was taken from each tube and added to 1 ml of Bio-Rad colorimetric assay solution. The assay solution contains Coomassie brilliant blue G-250 and changes color from deep red-brown to a bright blue in the presence of protein. Approximately ~1-2 ml of the fractions containing the most protein was collected and dialyzed at 4°C utilizing a 10,000 MWCO dialysis membrane (Spectra-Por CE). The dialysis tubing was clamped tightly on either end (two

clamps at each end), to ensure that no protein is lost during dialysis. 1 liter of fresh dialysis buffer was used for each dialysis step, and with each protein. First, the dialysis tubing with the protein sample was placed into Ni^{2+}-NTA column dialysis buffer A for 1 hour, followed by Ni^{2+}-NTA column dialysis in buffer B for 1-2 hours. Protein samples were then dialyzed overnight against Ni^{2+}-NTA column dialysis buffer B. The protein obtained in the final step was concentrated with an Amicon-Ultra cell concentrator (EMD Millipore) if needed. The protein was stored in a final solution of 50% dialysis buffer B and 50% glycerol (equal volume of glycerol). SDS-PAGE analysis was run following the purification and dialysis to confirm the purity of the protein. The Nano-Drop spectrophotometer was used to determine the protein concentration by measuring absorbance at 280 nm, using the "Protein" setting.

2.2.2.2.2 Protein purification by FPLC

With the goal of obtaining protein of high purity, *E. coli* BL21(DE3) cells containing recombinant protein, and harvested from ~250 ml of culture, were suspended in ~9.5 ml Ni^{2+} binding buffer. The binding buffer was added directly to the bottle with the cell pellet, and the bottle was kept on ice. To suspend the cells in solution, the mixture was swirled in the bottle, then poured into a 100 ml beaker and kept on ice throughout the process. The mixture was subjected to 1 min ultrasonic pulses (~5-6 watts; Misonix Inc), with cooling intervals of equivalent time (1 min) to ensure the solution was homogenous (~20-45 min). Low speed centrifugation (6000 rpm, 4°C) was then used to clarify the sonicated solution for 20-30 min. Ni-NTA affinity chromatography was carried out using the AKTA-FPLC Explorer system, utilizing a 1 ml His Trap^{TM} FF crude column (GE Healthcare) charged with $NiSO_4$ solution. Prior to purification all of the buffers used

were degassed for ~20 min and the column was always washed extensively with ddH_2O and 1M NaOH. The column was cleared with stripping buffer and recharged with $NiSO_4$ after every cycle of use. First the column was washed with ddH_2O (at least 10 column volumes or 10 ml), then binding buffer with TCEP added (~10 ml). Then the sample (~10 ml sonicated mixture) was loaded into the superloop. The FPLC program created for a transition from binding buffer to elution buffer was chosen, and the system would run the sample through the column. The binding buffer was connected to pump A, while the elution buffer was connected to pump B. Once the process was finished, the samples were kept on ice in a refrigerator until the next step was completed, as this was always carried out immediately following the initial purification. The AKTA-FPLC system was then washed (no reducing agent in any buffers for washing), stripped and recharged in the following manner: ddH_2O, followed by stripping buffer, then binding buffer, then ddH_2O. The column was then extensively washed (>1 hour) in NaOH, then ddH_2O, followed by binding buffer, ddH_2O, and ~1 ml $NiSO_4$ into the superloop in order to recharge the column. ~10 ml of each buffer or water was run through the system. Samples that were intended to be purified only by the His Trap™ FF crude column on the AKTA FPLC system, were eluted, dialyzed as described above, and stored in dialysis buffer B and 50% glycerol.

As an added measure of purification, an aliquot of sample that was FPLC purified, could also be desalted.

2.2.2.2.3 Desalting Purified Protein using the AKTA FPLC

Prior to desalting the AKTA FPLC-purified protein, the machine is conditioned to the specifications of the desalting process. The desalting process used a 5 ml HiTrap™ Desalting column (GE Healthcare). This column required washing with ~50 ml (10 column volumes) of each buffer. To condition the AKTA-FPLC and column to the buffers that would be used, ddH_2O is flushed through the entire system, followed by storage buffer, with TCEP added just prior to use. The sample obtained from the earlier crude purification column (normally ~1-2 ml) was loaded into the superloop of the system. The sample could be run on the desalting setting, with pump A in the storage buffer and pump B in ddH_2O. Once the desalting process was completed, the microcentrifuge tubes containing purified, desalted protein samples were placed on ice. Samples were stored in 50% glycerol solution (equal volume of glycerol added) at -20°C for immediate use, or -80°C for long term storage. The FPLC AKTA system was then programmed to flush the system, cleaning it first with ~50 ml of ddH_2O, followed by an extensive NaOH [0.2M] wash. Then, ddH_2O was used to wash the entire system, and the machine could then be stored by washing with 20% ethanol, ensuring full purging of the aparatus.

2.2.3 Enzyme Assays

2.2.3.1 R1.1 RNA Substrate Synthesis, Internal ^{32}P-Labeling and Purification

The R1.1 RNA used in cleavage assays was enzymatically synthesized using oligodeoxynucleotide templates that also encluded a T7 RNA polymerase Class III promoter sequence. The 77 nt R1.1 oligodeoxynucleotide (encoding R1.1 RNA; 60 nt) (6.75 µl used of 560 ng/µl concentration) and “G18 start” oligonucleotide promoter (18

nt) (1 µl of 1 µg/µl) were combined in a 100 µl volume annealing reaction with 10 mM Tris-HCl (pH 8.2). The sample was heated at 65°C for 5 min then cooled on ice. From this 100 µl total annealing reaction, a 10 µl aliquot of the template solution was used for the transcription reaction. The transcription reaction (100 µl total volume) contained 10 µl of the template solution from the annealing reaction, ~1 µg of T7 RNA polymerase, T7 transcription buffer (1X), 1 mM of each ribonucleoside 5'-triphosphate (rATP, rCTP, rGTP, and rUTP), and ~10-25 µCi of [α-^{32}P] UTP. The transcription reactions were incubated for 4 hours at 37°C. To stop the reactions, one-half volume of 7M urea-based gel loading solution containing bromophenol blue was added to the reaction. The sample was then electrophoresed in a 15% denaturing polyacrylamide gel as described above. Localization of the radiolabeled RNA was achieved by exposing the gel to X-ray film (Fuji RX) for 15 min. in the darkroom. The film was clipped at one corner to help with its orientation in respect to the gel, so that locating the gel region containing the RNA, with the gel situated in one corner of the cassette, was made more efficient. To develop the film, it was first placed in Kodak Developer Solution for 2 min, then in Kodak Stop solution for 1 min, and lastly the Kodak Fixing solution for 2 min (all from Sigma Aldrich). The visible and distinct dark band on the film was excised carefully with a scalpel, and then the film was placed onto the gel and oriented so that the empty excised region of the film sat precisely atop the actual RNA band in the gel. (The cut made earlier on the top of the film was useful at this point of the process to ensure proper orientation.) Using a sterile scalpel, the region of the gel containing the P^{32}-labeled R1.1 RNA was excised and crushed inside of a 1.5 ml polypropylene tube. The crushed gel slice was combined with ~600 µl of DNA/RNA extraction buffer for ~3-4 hours, followed by

centrifugation at 14,000 rpm for 30 min. The supernatant containing the RNA was transferred to a new tube and 1/10th volume of 3M ammonium acetate (pH 5.2) and 2.5 volumes of 100% ethanol were added, followed by careful mixing. The sample was held at -20°C overnight. Next, the sample was centrifuged at 14,000 rpm for 30 min. The RNA pellet was then carefully washed with 70% ethanol (aqueous) at room temperature. The pellet was centrifuged at 14,000 rpm for 15 min. The pellet was air dried to remove residual ethanol. The P^{32}-labeled R1.1 RNA was suspended in 100 µl TE buffer and stored at -20°C.

In a LS6500 liquid scintillation counter (Beckman-Coulter), 1 µl of radiolabeled RNA sample in ~7 ml liquid scintillation solution (Scintiverse) was used to detect the amount of counts per minute (cpm) given off by the R1.1 RNA. The cpm value can then be used to calculate the amount of radiolabeled RNA that will be used in various analyses. The equation to convert cpm to mmol RNA is below:

$$= \frac{\text{CPM/Counting efficiency (0.99)}}{\left[\frac{\text{Number of U residues in strand X µCi of hot UTP used X (2.2X 10}^6\text{ dpm/µCi)}}{\text{Total mmol of cold UTP used}}\right]}$$

2.2.3.2 Substrate cleavage assays

RNA cleavage assays were performed using internally ^{32}P-labeled R1.1 RNA. For all time course assays, master reactions (40 µl) were prepared, and at each time point, 10 µl was removed and mixed into a 0.65 ml microcentrifuge tube containing the reaction stop mix (4X) in the proper amount (~2.5-3 µl). Ec-YmdB RNA cleavage assay master reaction mixes were pre-incubated for 5 min at 37°C prior to RNA addition. 4X stop mix containing SDS was used to quench the YmdB reactions, achieving a 1X final

concentration. For the Ec-RNase III time-course assay of R1.1 RNA cleavage, a different RNase III-specific cleavage reaction buffer was used that contained $MgCl_2$, as RNase III requires a divalent metal cation for ribonucleolytic activity. The RNase III cleavage reaction was also incubated at 37°C for 5 min prior to starting the time course cleavage assay. The RNase III reactions were quenched by adding a half volume of (2X) Stop Mix containing excess EDTA. 15% denaturing polyacrylamide gels containing 7 M urea were used to analyze the reactions. Gels were run in 1X TBE buffer for ~ 90 min at a constant voltage of ~300 V. Gels were exposed to a phosphoimager screen overnight at 4°C. The Typhoon 9400 Phosphorimager System was used to scan the phosphorimager screen, and the ImageQuantTL program was used for image analysis.

Table 1. List of the oligonucleotides and mutagenic primers used.

Oligonucleotide name	**Sequence (5'→3')**
G18 Start (T7 promoter oligo)	TAATACGACTCACTATAG
R1.1 (T7 phage R1.1 RNA)	AAGAAGGTCAATCATAAAGGCCACTCTTGCG AATGACCTTGAGTTTGTCCCTCTACTCCCC
Ec-YmdB Wild-Type	ACTGGGGTTTATGGTTTCCCT**AGG**GCGG CAGCGGCTGAAATCGCA
Ec-YmdB R130A primer	GATTTCACCGCTGCC**GCA**GCAGGGTAAC CATAAAC
Ec-YmdB R130K primer	ACTGGGGTTTATGGTTTCCCT**AAG**GCGGC AGCGGCTGAAATCGCA
Ec-YmdB R130E primer	ACTGGGGTTTATGGTTTCCCT**GAG**GCGGCAGCG GCTGAAATCGCA
Ec-YmdB D11A primer	CATGTTGTGCAGGGT**GCT**ATTACCAAACTGGCC
Ec-YmdB D11K primer	CATGTTGTGCAGGGT**AAA**ATTACCAAACTGGCC
Ec-YmdB D11E primer	CATGTTGTGCAGGGT**GAA**ATTACCAAACTGGCC

CHAPTER 3
RESULTS AND DISCUSSION

3.1 Ribonucleolytic activity of YmdB

Previous enzymatic cleavage assays conducted in the Nicholson laboratory at Temple University had found that purified *Ec*-YmdB exhibits ribonucleolytic activity towards the model 60 nt RNA, R1.1 RNA (Paudyal, 2014). *Ec*-YmdB and the *Ec*-YmdB D160A mutant, both had shown ribonucleolytic activity in a manner independent of RNase III, and with the D160A mutant able to cleave R1.1 in a manner insensitive to high salt concentrations (Paudyal, 2014). This novel finding led to the investigations in this project, with the goal of characterizing features of YmdB important for ribonucleolytic activity.

3.1.1 YmdB cleavage capabilities

The *Ec*-YmdB used in this project was purified using either an AKTA FPLC system with a 1 ml HisTrap TM FF crude Ni^{2+} column, or by gravity flow through a Ni^{2+} affinity chromatography column (Figs. 4 and 5). The protein was then dialyzed and/or desalted to create the appropriate storage buffer conditions. It is important to note that the gravity-purified proteins used in the cleavage assays in this project were purified following the protocol carried out by S.P. (Paudyal, 2014). In addition, a number of protocols were followed to assess protein purity and ensure that protein samples were collected properly. These included SDS-PAGE, Bio-Rad colorimetric assays, and the Unicorn software program in tandem with the AKTA FPLC.

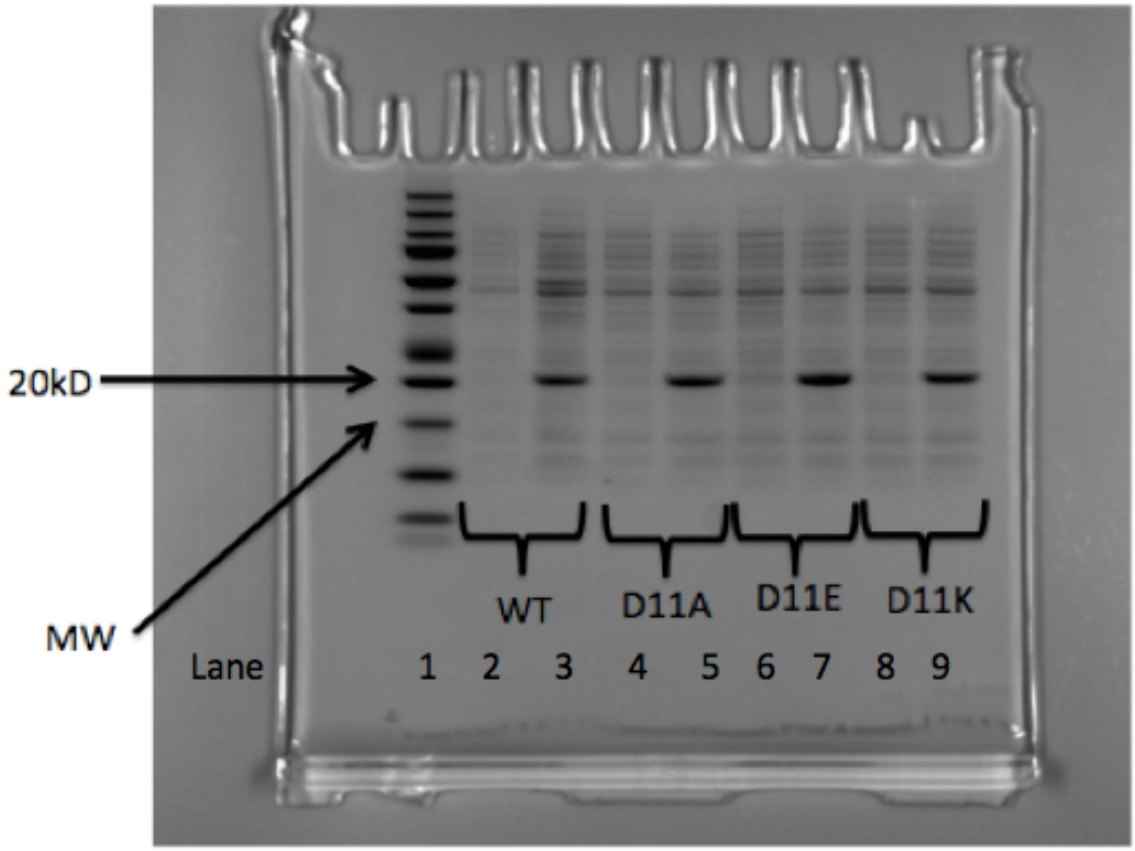

Figure 4: IPTG-dependent production of recombinant (His)$_6$ *Ec*-YmdB (wild type and D11 mutants) protein in *E. coli* BL21(DE3) cells.
BL21(DE3) *E. coli* cells containing recombinant pET-15b plasmids were grown in LB-broth (500 ml) with ampicillin at 37˚C to an optical density of 0.4 at ~595 nm (~2-4 hours). IPTG (1 mM final concentration) was added to induce protein expression, and cell growth continued for 4 hours. Aliquots (1 ml) were removed before and 4 hours post IPTG induction, and analyzed by SDS-PAGE.
Lane 1: protein size markers (Precision Plus Protein Dual Xtra markers; 10 µl). Sample lanes (2 – 9) each held 5 µl of pre- or post-IPTG addition sample, combined with 5 µl of 2X denaturing gel loading buffer with 2-mercaptoethanol. Samples were heated prior to loading. Lane 2: wild-type (WT) *Ec*-YmdB prior to IPTG addition; Lane 3: wild-type (WT) *Ec*-YmdB 4 hours after IPTG addition; Lane 4: D11A *Ec*-YmdB prior to IPTG addition; Lane 5: D11A *Ec*-YmdB 4 hours after IPTG addition; Lane 6: D11E *Ec*-YmdB before IPTG addition; Lane 7: D11E *Ec*-YmdB 4 hours after IPTG addition; Lane 8: D11K *Ec*-YmdB pre-IPTG addition; Lane 9: D11K *Ec*-YmdB 4 hours post IPTG induction.

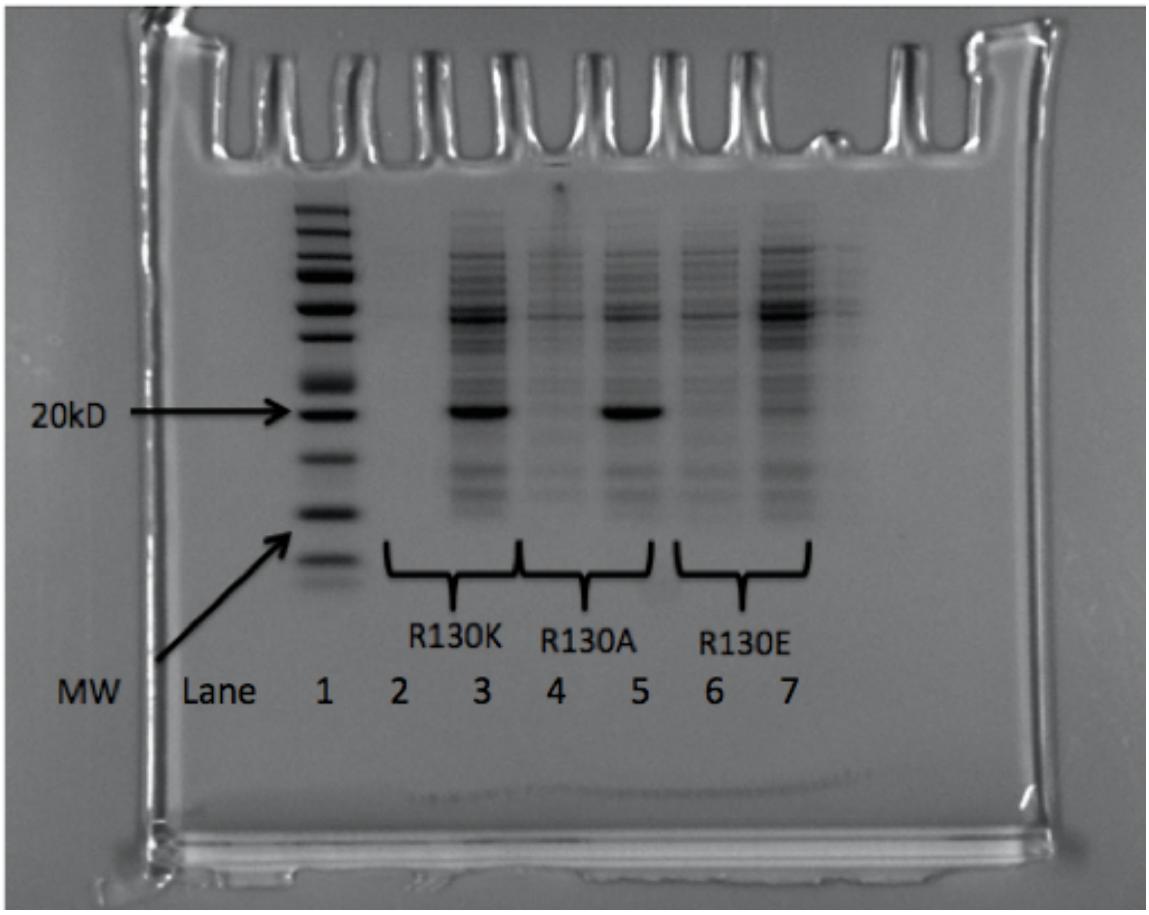

Figure 5. IPTG-dependent production of $(His)_6$ *Ec*-YmdB R130 mutant proteins in *E. coli* BL21(DE3) cells.

E. coli BL21(DE3) cells containing recombinant pET-15b plasmids were grown in 500 ml LB-broth with ampicillin at 37˚C to an optical density of 0.4 at ~595 nm (~2-4 hours). IPTG (1 mM final concentration) was then added to induce recombinant protein overexpression. The culture was incubated with shaking for 4 hours post IPTG induction. Aliquots (1 ml) pre- and post-IPTG induction were removed for SDS-PAGE analysis. Lane 1: Precision Plus Protein Dual Xtra markers (10 µl). Lanes 2-7 each held 5 µl of pre- or post-IPTG induction samples combined with 5 µl of 2X Denaturing Gel Loading Buffer with 2-mercaptoethanol. Lane 2: R130K *Ec*-YmdB pre-IPTG addition; Lane 3: R130K *Ec*-YmdB 4 hours post IPTG addition; Lane 4: R130A *Ec*-YmdB pre-IPTG addition; Lane 5: R130A *Ec*-YmdB 4 hours Post IPTG induction; Lane 6: R130E *Ec*-YmdB pre-IPTG addition; Lane 7: R130E *Ec*-YmdB 4 hours post IPTG addition.

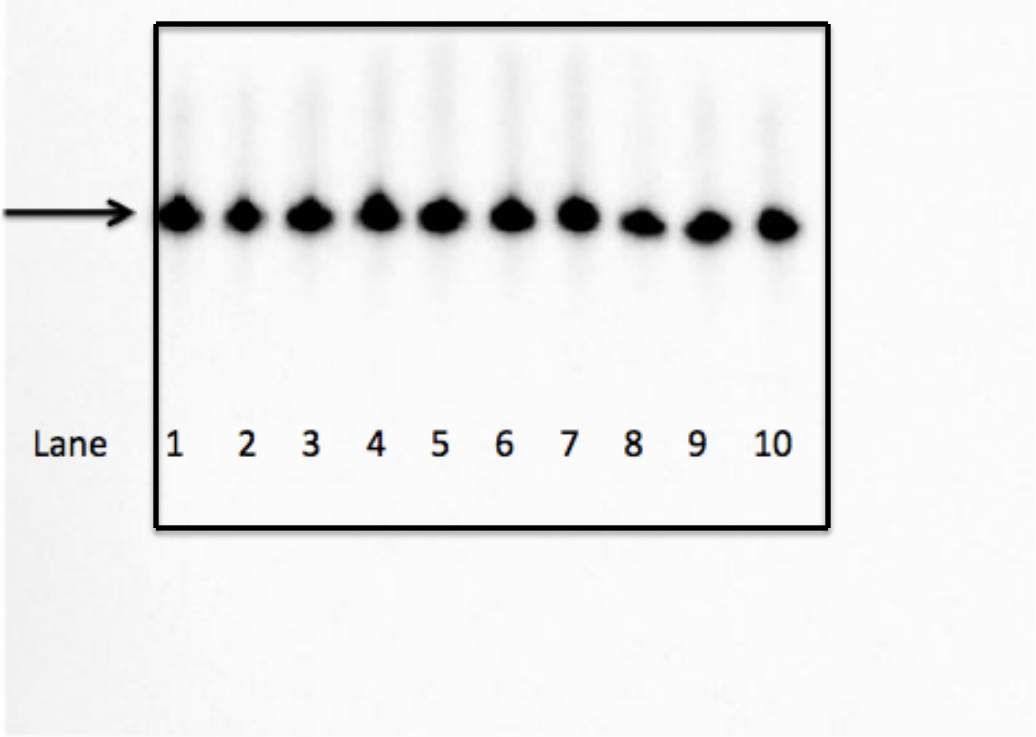

Figure 6: Ribonucleolytic cleavage of R1.1RNA by *Ec*-YmdB wild-type protein.

The reaction conditions were as follows: The R1.1 RNA cleavage assay buffer consisted of 30 mM Tris-HCl (pH 8.0), 40 mM NaCl, 100nM internally ^{32}P-labeled R1.1 RNA. The protein concentration was 250 nM. Reactions were incubated at 37°C for 0, 15, and 30 minutes. 10 µl of the total reaction was loaded into each lane of a denaturing 15% polyacrylamide gel, containing TBE buffer. Electrophoresis was carried out at ~300 volts. Lane 1: R1.1 RNA incubated for 30 minutes without protein. Lanes 2-4 show a time course assay for HisBind gravity column purified WT *Ec*-YmdB protein and incubated for 0, 15 and 30 minutes. Lanes 5-7 show a time course assay for WT *Ec*-YmdB protein purified by Fast Protein Liquid Chromatography (AKTA FPLC) and incubated for 0, 15 and 30 minutes. Lanes 8-10 show a time course assay for WT *Ec*-YmdB protein purified by Fast Protein Liquid Chromatography (AKTA FPLC), followed by desalting using the AKTA system.

In this project, wild-type *Ec*-YmdB that was purified by three different protocols lacked demonstrable ribonucleolytic activity, in contrast to previous analyses described above (Fig. 6). In these analyses, reactions were carried out at pH 8.0 and pH 7.5, with no difference in WT *Ec*-YmdB activity.

To evaluate whether R1.1 RNA was properly synthesized, previously purified *Ec*-RNase III was used to test the substrate competence. R1.1 RNA is an authentic, well-characterized substrate of *Ec*-RNase III. The RNase III exhibited the expected ribonucleolytic cleavage pattern for the R1.1 RNA (Fig. 7), consisting of a (strong) primary cleavage site, and a (weaker) secondary site. This finding ruled out the

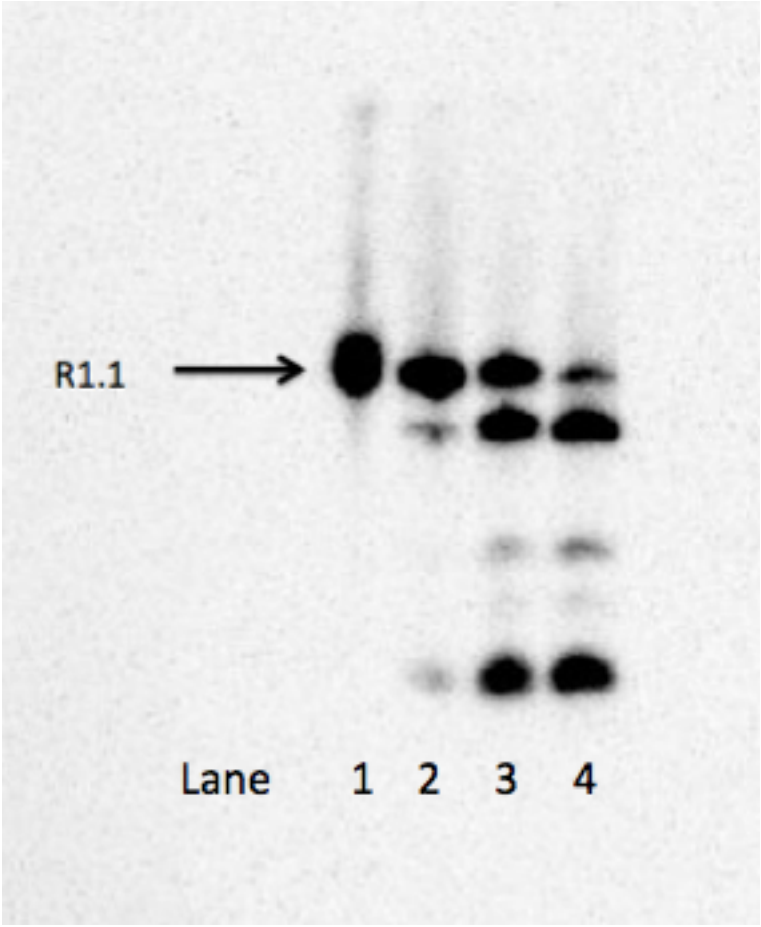

Figure 7. Cleavage of R1.1 RNA by *Ec*-RNase III.
Ec-RNase III cleavage assay buffer consisted of 30 mM Tris-HCl (pH 8.0) and 160 mM NaCl. All reactions had an internally ^{32}P-labeled R1.1 RNA concentration of 100 nM. 10µl aliquots of the total reactions were electrophoresed on a 15% polyacrylamide gel with 7 M urea and TBE buffer at ~300 volts. $(His)_6$-*Ec*-RNase III protein (purified previously) was incubated with internally ^{32}P-labeled R1.1 RNA. Reactions were incubated at 37°C for 0 (Lane 2), 15 (Lane 3), and 30 minutes (Lane 4). Lane 1 is a control, where R1.1 RNA was incubated for 30 min without protein.

possibility that the R1.1 RNA synthesized for this project was resistant to cleavage by WT *Ec*-YmdB due to structural flaws.

To investigate why the Ec-YmdB proteins purified for this project did not exhibit the ribonucleolytic activity observed in analyses carried out by S.P., the WT *Ec*-YmdB and D160A *Ec*-YmdB mutant protein (both purified by S.P.) were directly compared with YmdB proteins purified for this project by SDS-PAGE (Fig. 8). This analysis showed no difference in molecular weight or purity when comparing the WT *Ec*-YmdB proteins purified by the Ni-NTA gravity flow column.

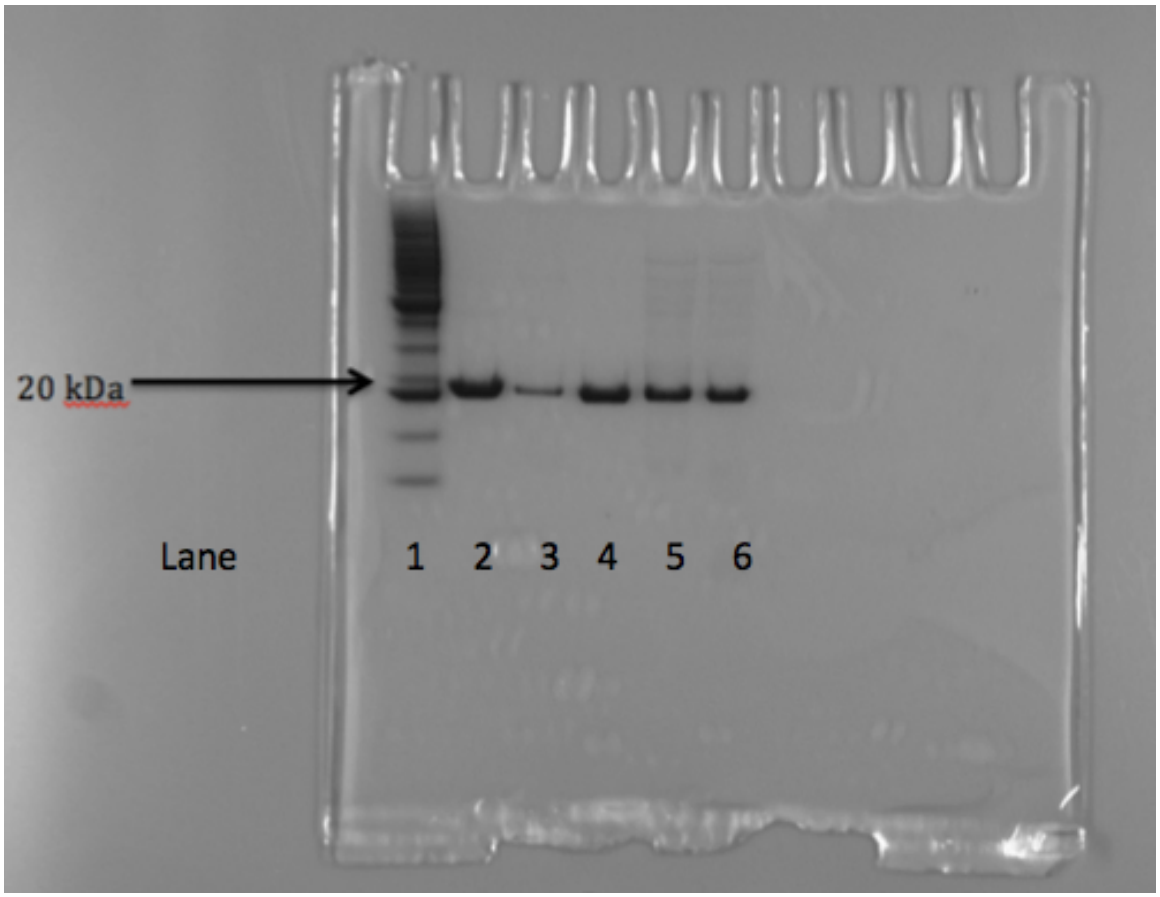

Figure 8. SDS-PAGE analysis of purified $(His)_6$ *Ec*-YmdB proteins

A 12% SDS-PAGE was used to assess the purity of the wild type $(His)_6$-*Ec*-YmdB protein purified for this project, compared to a sample previously purified by S.P. Lane 1: Protein molecular weight standards; Lane 2: Wild type His_6-*Ec*-YmdB purified by S.P.; Lane 3: D160A mutant protein purified by S.P.; Lane 4: Wild- type His_6-*Ec*-YmdB freshly purified by nickel-NTA ("HisBind") gravity column; Lane 5: Wild-type His_6-*Ec*-YmdB purified by Fast Protein Liquid Chromatography (FPLC). Lane 6: Wild-type His_6-*Ec*-YmdB freshly purified by Fast Protein Liquid Chromatography (AKTA-FPLC) using a Hi-Trap Ni-NTA affinity column, followed by a desalting.

The previously purified Ec-YmdB proteins that originally exhibited ribonucleolytic activity towards R1.1 continued to demonstrate cleavage activity (Fig. 9). The freshly purified wild type *Ec*-YmdB, purified using three different methods, as described in this paper, continued to show a lack of ribonucleolytic activity towards the R1.1 substrate (Fig. 6). The cleavage assay carried out using

proteins previously purified by S. P., confirms that the lack of cleavage activity exhibited by freshly purified WT *Ec*-YmdB was not due to a technical error or a miscalculation when setting up cleavage assays, as the standard protocol was followed for all of the experiments performed.

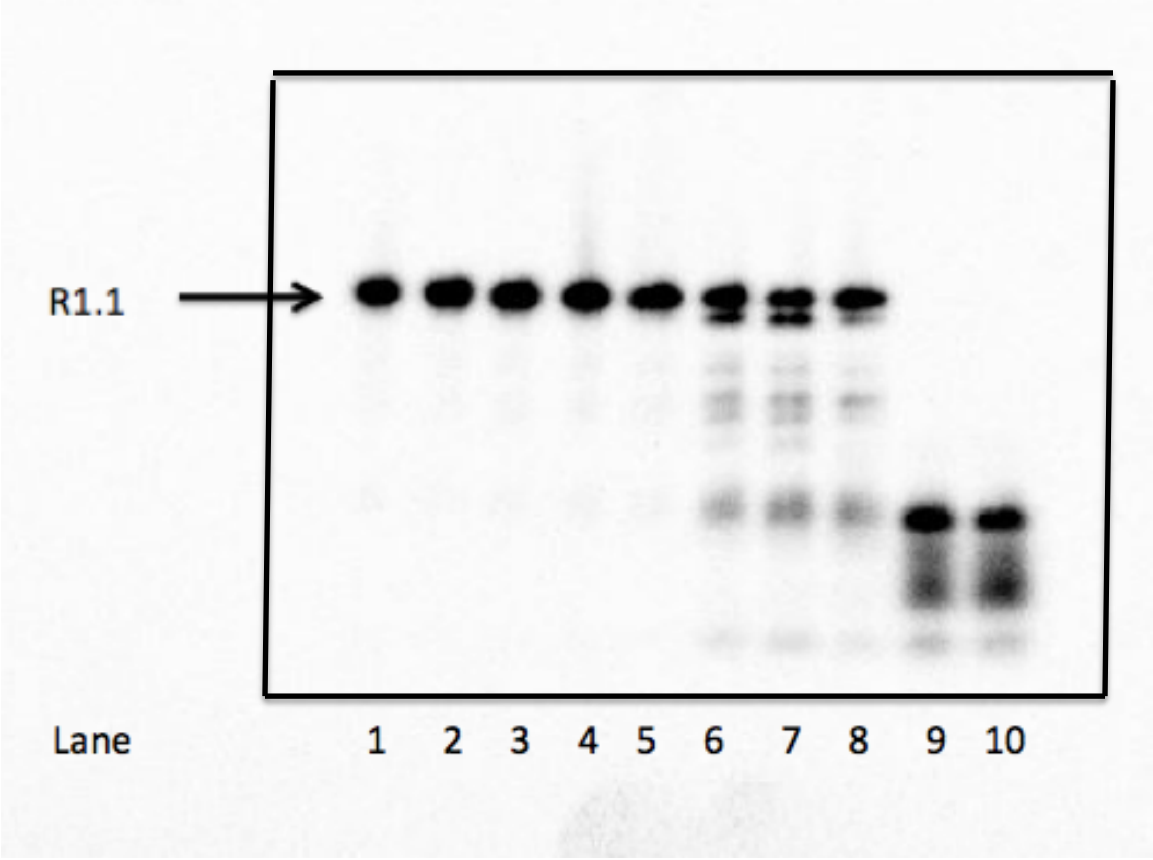

Figure 9. Ribonucleolytic activity of *Ec*-YmdB and D160A mutant.

The *Ec*-YmdB cleavage assays contained 30 mM Tris-HCl (pH 8.0), 40 mM NaCl, 100 nM R1.1RNA and 250nM *Ec*-YmdB. Reactions were incubated at 37°C for 0, 30, and 60 minutes. 7.5µl from each reaction was analyzed by 15% SDS-PAGE. Lane 1: R1.1 RNA incubated 60 minutes without protein. Lanes 2-4: time course assay for *Ec*-YmdB protein, purified by nickel gravity (HisBind) column for this project.; Lanes 5-7: time course assay for *Ec*-YmdB protein purified by S. P. *via* nickel gravity column; Lanes 8-10: time course assay for the *Ec*-YmdB D160A mutant purified *via* nickel gravity column by S. P.

Multiple *Ec*-YmdB mutants were created in this project in order to analyze the effects of mutating individual, single amino acid residues on R1.1 cleavage by *Ec*-

YmdB. The positions of R130 and D11 were selected for mutagenesis in this study because of their high conservation and location either within the adenine binding pocket (D11), or near the pocket (R130). The specific amino acid substitutions introduced at D11 and R130 were chosen to analyze the effect of both side chain size and charge on YmdB ribonucleolytic activity. D11, positioned in the adenine binding pocket, is implicated in binding the adenine base by two hydrogen bonds. Three mutations changed D11 to an alanine (D11A), a glutamic acid (D11E), or a lysine (D11K). Three mutations that were substituted at position R130 were alanine (R130A), glutamic acid (R130E), and lysine (R130K).

The D11K mutation changed a negatively charged residue to a positively-charged residue. The R130E mutation substituted a positively charged residue to a negatively charged residue. The R130E and D11K Ec-YmdB recombinant proteins were not able to be produced in BL21(DE3) cells. Notably, specific bands associated with these mutants were not observed by SDS-PAGE. Hence, the R130E and D11K mutant proteins were not analyzed further. The D11E mutant retains a negative charge but with a larger side chain; the R130K mutant retains a positive charge but again has a larger, more complex side chain. The D11A and R130A mutations were created in an attempt to view complete loss of charge (along with steric size reduction) at those specific locations.

R1.1 RNA cleavage assays were performed using the four different *Ec*-YmdB mutant proteins (D11A, D11E, R130A, R130K), following the same standard protocol performed with wild type *Ec*-YmdB. Reactions were analyzed using denaturing 15% polyacrylamide gels. The cleavage assays performed using the

D11A and D11E mutants exhibited a defined cleavage pattern (Fig. 10). The D11A mutant produced a strong, well-defined cleavage pattern. The FPLC-purified D11E mutant also produced a visible, defined cleavage pattern, though not as strong as that seen with the D11A mutant, leading to the conclusion that the R1.1 RNA was not cleaved as readily by D11E YmdB as it was by D11A YmdB protein. The introduction of a single methylene group (aspartic acid (D) to alanine (A)) was sufficient to allow *Ec*-YmdB to cleave R1.1 RNA in the experimental conditions used. Removal of the carboxylic acid group (aspartic acid to alanine) appeared to provide stronger activation.

The R130A and R130K mutants were both purified and used in time course cleavage assays with R1.1 RNA, following the same protocol. Neither mutation led to any difference in ribonucleolytic activity compared to WT-*Ec*-YmdB (Fig 11). The lack of any activation of ribonucleolytic activity suggests that this residue does not directly influence RNA cleavage by *Ec*-YmdB. Nonetheless, residue R130 can still potentially play an important role for YmdB function, since inclusion bodies were dramatically observable in the R130E mutant, suggesting that R130 could have a role in the folding and structural integrity of *Ec*-YmdB. (Inclusion bodies were also apparent with the D11K mutant.)

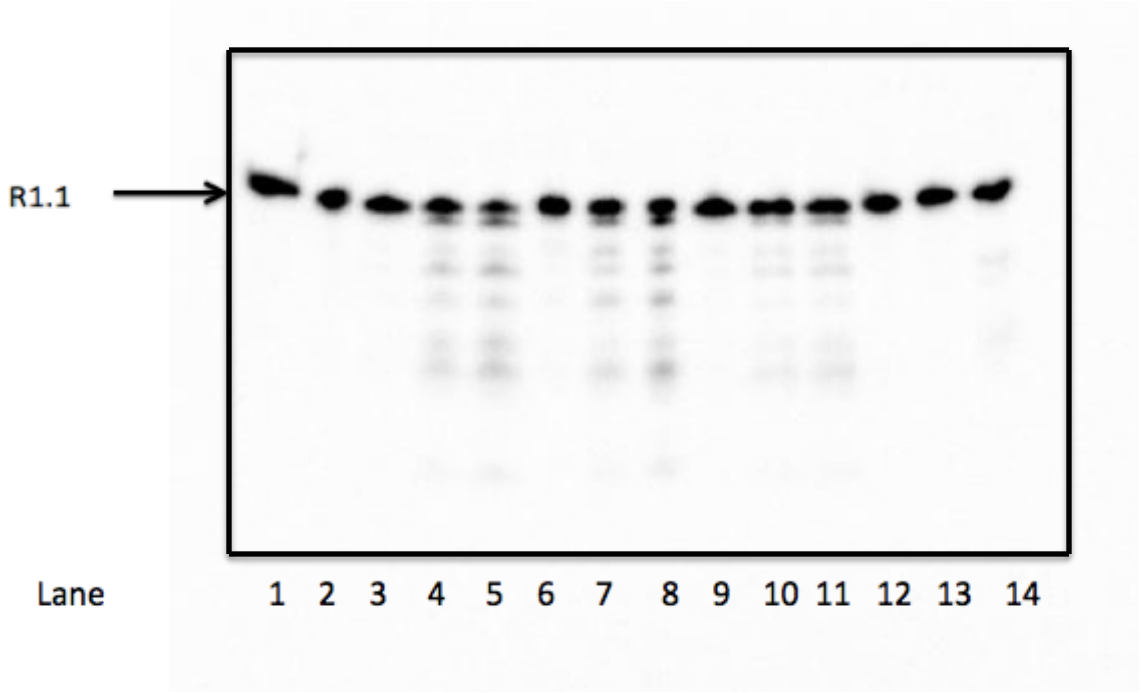

Figure 10. Ribonucleolytic activity of the D11A and D11E *Ec*-YmdB mutants.

The *Ec*-YmdB cleavage assays contained 30 mM Tris-HCl (pH 8.0), 40 mM NaCl, 100 nM R1.1RNA and 250nM *Ec*-YmdB. Reactions were incubated at 37°C for 0, 30, and 60 minutes. 7.5µl from each reaction was analyzed by 15% SDS-PAGE. $(His)_6$-*Ec*-Ymdb wild type and D11 mutated proteins used in these assays were purified through various methods. Lane 1: R1.1 RNA incubated 30 minutes without protein; Lane 2: cleavage reaction (30 min.) with gravity purified WT *Ec*-YmdB. Lanes 3 through 14 show the results of time course cleavage assays carried out for 0, 15, and 30 minutes. Lanes 3-5: Ec-YmdB D11A purified by nickel gravity column; Lanes 6-8: Ec-YmdB D11A purified by Fast Protein Liquid Chromatography (FPLC); Lanes 9-11: Ec-YmdB D11E purified by nickel gravity column; Lanes 12-14: Ec-YmdB D11E purified by Fast Protein Liquid Chromatography (FPLC).

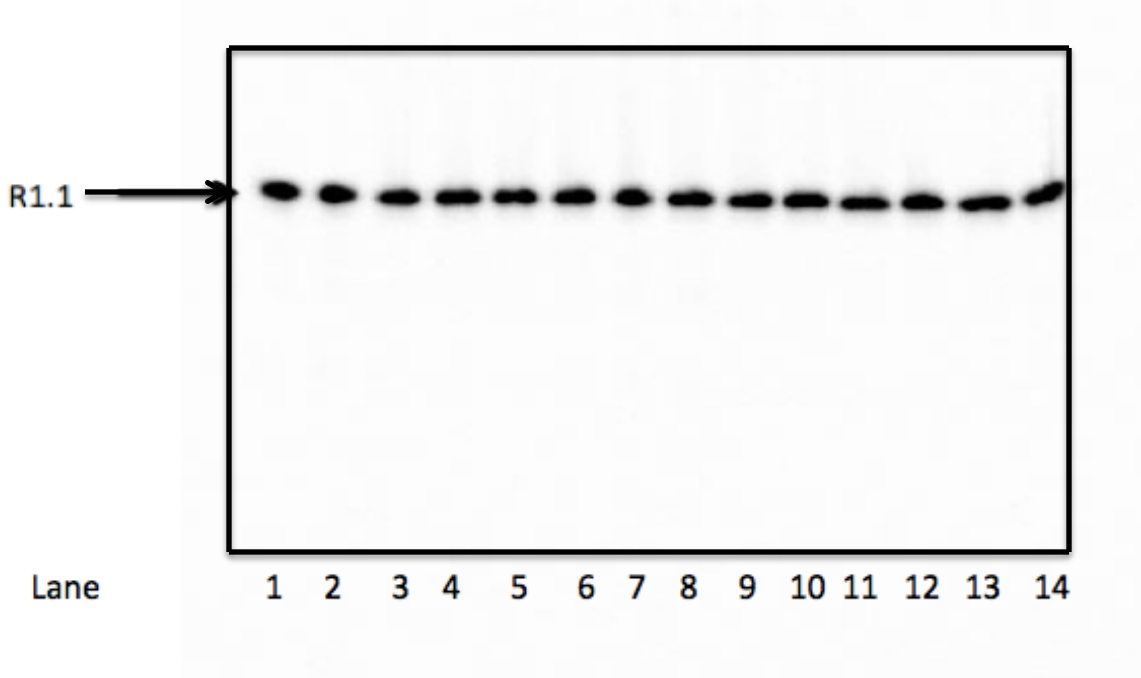

Figure 11. Absence of ribonucleolytic activity of the *Ec*-YmdB R130K and R130A mutants.

The *Ec*-YmdB R130A and R130A mutant cleavage assays contained 30 mM Tris-HCl (pH 8.0), 40 mM NaCl, 100 nM R1.1RNA and 250nM *Ec*-YmdB. Reactions were incubated at 37°C for 0, 30, and 60 minutes. 7.5µl from each reaction was analyzed by 15% SDS-PAGE. $(His)_6$-*Ec*-Ymdb wild type and R130 mutated proteins used in these assays were purified through various methods. Lane 1: R1.1 RNA incubated 30 minutes without protein; Lane 2: cleavage reaction (30 min.) with gravity purified WT *Ec*-YmdB. Lanes 3 through 14 show the results of time course cleavage assays carried out for 0, 15, and 30 minutes. Lanes 3-5: Ec-YmdB R130K purified by nickel gravity (HisBind) column; Lanes 6-8: R130K purified by Fast Protein Liquid Chromatography (FPLC) using a HiTrap column; Lanes 9-11: R130A purified by nickel gravity (HisBind) column; Lanes 12-14: R130A mutant, purified by Fast Protein Liquid Chromatography (FPLC).

3.1.2 Involvement of the YmdB adenine binding pocket in ribonucleolytic activity.

Ec-YmdB residue D11 has an important function in the ADPR-binding pocket. The macrodomain of YmdB has a very similar structure and function found across many species, including the nsP3 protein of Chikungunya virus (CHIKV) which shows strong structural similarity. As mentioned, the CHIKV nsP3 protein has residue D10, which is equivalent to D11 in *Ec*-YmdB. In CHIKV, nsP3 is able to bind rAAA (ribotriphosphate), with the central adenine accommodated in the RNA-binding pocket. in YmdB, the adenine of OAADPR is expected to bind the D11 residue. Deacetylation can then proceed, yielding ADPR and acetate. Another possibility is that the macrodomain binding site could accommodate other adenine-containing small molecules, which regulate YmdB function. Thus, the macrodomain may not be entirely ADPR-specific.

Specific amino acid substitutions at position D11 lead to *Ec*-YmdB ribonucleolytic activity. In contrast, mutations at position R130 did not activate RNA cleavage. Thus, the change in cleavage activity with the D11 mutations was site-specific. The D11E mutation changed the aspartic acid, to glutamic acid which has a larger, though still negatively charged, side chain. The cleavage activity observed by this mutant could result from a conformational distortion of the ADPR-binding pocket due to the larger side chain that replaced the residue in the wild type structure. The D11A mutation changed the negatively charged aspartic acid in the wild type YmdB to a neutral alanine with a small methyl group as a side chain. This change led to robust ribonucleolytic activity. The ribonucleolytic activity of this

mutant could occur due to additional space in the ADPR-binding pocket, allowing other small molecule metabolites to interact in the site.

It has been observed in other proteins that catalytic sites are able to bind a range of substrates. Specifically, the human ssDNA-binding protein 1 (hSSB1) has an oligonucleotide/oligosaccharide-binding (OB) fold that has a tendency to bind RNA or DNA that is single-stranded (Zhang et al. 2013). The OB fold of hSSB1 was unexpectedly found to demonstrate a high affinity for poly (ADP ribose; PAR) and also recognized *iso*-ADPR, but not *mono*-ADPR (Zhang et al. 2013). Reviewing the results of this experiment, while considering previous findings from another protein, the D11 residue within the macrodomain adenine-binding pocket of *Ec*-YmdB could indeed play a pivotal role in not only promoting OAADPR deacetylation, but perhaps also in recognition, and cleavage of specific RNA sequences.

Why there is a difference in ribonucleolytic activity between the WT *Ec*-YmdB that was previously purified, and the freshly purified WT *Ec*-YmdB is yet to be determined. Taking into consideration the potentially broader range of molecules that could be interacting with the adenine-binding pocket, apart from OAADPR or ADPR, other metabolites could also play a role. As Zhang et al. (2013) found, monomeric and isomeric forms of ADPR were recognized by the "OB fold" of hSSB1 in a significantly different way, which had a large impact on the mobilization of hSSB1 to locations of DNA damage, which in turn can cause mutational changes.

SUMMARY

This project has shown that specific mutant forms of *Ec*-YmdB have the capacity to cleave RNA, and that the two mutations involve a conserved residue in a conserved adenine-binding pocket. Residue 11 in *Ec*-YmdB appears to be integral to the regulation of the ribonucleolytic activity.

Newly-purified wt *Ec*-YmdB did not show ribonucleolytic activity, however, a single mutation of a negatively charged residue [at position D11] allowed RNA cleavage, and leads to many added possibilities for the role of that residue. It can be postulated that a monomeric or isomeric form of a metabolite, possibly related to ADPR, may be important for the observed activity, as was mentioned by Zhang et al. (2013). Previous studies involving YmdB focused on monitoring its inhibitory effect upon RNase III. In these studies the YmdB is incubated with RNA alone but there was no RNA cleavage observed (Kim, Manasherob, 2008). The difference in ribonucleolytic activity observed between the previously purified wild type *Ec*-YmdB and the freshly purified versions of wild type *Ec*-YmdB could be due to the presence of a metabolite from the cells the protein was extracted from, that caused the previous wild type YmdB to cleave ssRNA.

Based on the results described herein, it is clear that the adenine-binding pocket of the YmdB macrodomain has an effect on the ribonucleolytic activity of YmdB. Future experiments are planned that will examine whether ADPR presence, concentration, or monomeric or isomeric forms play any role in the ribonucleolytic activity of YmdB.

Supplemental Figure

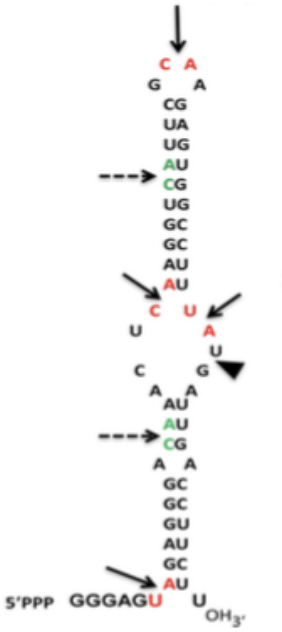

Figure S1: R1.1 RNA structure with proposed cleavage sites for Ec-YmdB.
The arrows indicate possible cleavage sites within the R1.1 RNA structure for Ec-YmdB cleavage. YmdB is assumed to preferentially cleave 5'-UpA-3' or 5'-CpA-3' dinucleotide motifs (red). The two dashed arrows indicate CpA (green) sequences in the areas that are expected to exhibit double stranded structure, which would be expected to experience less reactivity towards YmdB. If the R1.1 RNA was to be completely cleaved in all sites then 7 products would be produced. The arrowhead indicates an RNase III cleavage site within the R1.1 RNA. (Paudyal, 2014)

REFERENCES

Alberts, B., Johnson, A., Lewis, J., Raff, M., Roberts, K., Walter, P. (2007). Molecular Biology of the Cell. New York: NY.

Butland, G., J. M. Peregrin-Alvarez, J. Li, W. Yang, X. Yang, V. Canadien, A. Starostine, D. Richards, B. Beattie, N. Krogan, M. Davey, J. Parkinson, J. Greenblatt and A. Emili (2005). "Interaction network containing conserved and essential protein complexes in Escherichia coli." Nature (London, U. K.) 433(7025): 531-537.

Chen, D., M. Vollmar, M. N. Rossi, C. Phillips, R. Kraehenbuehl, D. Slade, P. V. Mehrotra, F. von Delft, S. K. Crosthwaite, O. Gileadi, J. M. Denu and I. Ahel (2011). "Identification of Macrodomain Proteins as Novel O-Acetyl-ADP-ribose Deacetylases." J. Biol. Chem. 286(15): 13261-13271.

Crick, F. H. C. (1970). "Central dogma of molecular biology." Nature (London) 227(5258): 561-563.

Guzman, D. L., Randall, A., Baldi, P., and Guan, Z. (2010 “Computational and single-molecule force studies of a macro domain protein reveal a key molecular determinant for mechanical stability.” PNAS. 107 (5): 1989-1994.

Han, W., X. Li and X. Fu (2011). "The macro domain protein family: Structure, functions, and their potential therapeutic implications." Mutat. Res., Rev. Mutat. Res. 727(3): 86-103.

Harvey Lodish , A. B., Lawrence Zipursky , Paul Matsudaira, David Baltimore, James Darnell (2000). Molecular Cell Biology. New York: NY, WH Freeman.

Hu, P., S. C. Janga, M. Babu, J. J. Diaz-Mejia, G. Butland, W. Yang, O. Pogoutse, X. Guo, S. Phanse, P. Wong, S. Chandran, C. Christopoulos, A. Nazarians-Armavil, N. K. Nasseri,

G. Musso, M. Ali, N. Nazemof, V. Eroukova, A. Golshani, A. Paccanaro, J. F. Greenblatt, G. Moreno-Hagelsieb and A. Emili (2009). "Global functional atlas of Escherichia coli encompassing previously uncharacterized proteins." PLoS Biol. 7(4): 0929-0947.

Huang, N., J. De Ingeniis, L. Galeazzi, C. Mancini, Y. D. Korostelev, A. B. Rakhmaninova, M. S. Gelfand, D. A. Rodionov, N. Raffaelli and H. Zhang (2009). "Structure and function of an ADP-ribose-dependent transcriptional regulator of NAD metabolism." Structure 17(7): 939-951.

Jankevicius, G., M. Hassler, B. Golia, V. Rybin, M. Zacharias, G. Timinszky and A. G. Ladurner (2013). "A family of macrodomain proteins reverses cellular mono-ADP-ribosylation." Nat. Struct. Mol. Biol. 20(4): 508-514.

Kim, K.-s., R. Manasherob and S. N. Cohen (2008). "YmdB: a stress-responsive ribonuclease-binding regulator of E. coli RNase III activity." Genes Dev. 22(24): 3497- 3508.

Kim, T., Lee, J., and Kim, K. (2013). “Escherichia coli YmdB regulates biofilm formation independently of its role as an RNase III modulator”. BMC Microbiology 13:266

Kraus, W. L. (2009). "New functions for an ancient domain." Nature Structural & Molecular Biology 16(9): 904-907.

Malet, H., Coutard, B., Jamal, S., Dutartre, H., Papageorgiou, N., Neuvonen, M., Ahola, T., Forrester, N., Gould, E. A., Lafitte, D., Ferron, F., Lescar, J., Gorbalenya, A. E., de Lamballerie, X., and Canard, B. (2009). “The Crystal Structures of Chikungunya and Venezuelan Equine Encephalitis Virus nsP3 Macro Domains Define a Conserved Adenosine Binding Pocket”. Journal of Virology 83(13): 6534-65-45

Neuvonen, M., and Ahola, T. (2009) “Differential Activities of Cellular and Viral Macro Domain Proteins in Binding of ADP-Ribose Metabolites”. Journal of Molecular Bioogy. 385(1): 212-225.

Nicholson, A. W. (2003). The ribonuclease III superfamily: forms and function in RNA maturation, decay, and gene silencing. In RNAi: A Guide to Gene Silencing. G. Hannon. NY, Cold Spring Harbor Laboratory Press. 149-174.

Nicholson, A. W. (2013). "Ribonuclease III mechanisms of double-stranded RNA cleavage." Wiley Interdiscip Rev RNA.

Paudyalm S., Alfonso-Prieto, M., Carnevale, V., Redhu, S. K., Klein, M. L., and Nicholson, A. W. (2015). “Combined computational and experimental analysis of a complex of ribonuclease III and the regulatory macrodomain protein, YmdB.” Proteins 83:459-472.

Peterson, F. C., Chen, D., Lytle, B. L., Rossi, M. N., Ahel, I., Denu, J. M., Volkman, B. F. (2011). “Orphan macrodomain (human C6ORF130) is an o-acyl-ADP-ribose deacylase: solution structure and catalytic properties.” J. Biol. Chem.

Pray, L. (2008) Discovery of DNA structure and function: Watson and Crick. Nature Education 1(1):100.

Tong, L. and J. M. Denu (2010). "Function and metabolism of sirtuin metabolite O-acetyl-ADP-ribose." Biochim. Biophys. Acta, Proteins Proteomics 1804(8): 1617-1625.

Wagner, S., Klepsch, M. M., Schlegel, S., Appel, A., Draheim, R., Tarry, M., Högbom, M., van Wijk, K. J., Slotboom, D. J., Persson, J. O., and de Gier J.
Tuning Escherichia coli for membrane protein overexpression. (2008).

Zhang, H., Kolb, F.A., Jaskiewicz, L., Westhof, E., and Flipowicz, W. 2004. Single processing center models for human Dicer and bacterial RNase III. Cell 118: 57–68.